Theses and Dissertations   Student Graduate Works

3-2002

Fretting Fatigue Behavior of a Titanium Alloy Ti-6AL-4V at Elevated Temperature

Onder Sahan

**FRETTING FATIGUE BEHAVIOR OF A
TITANIUM ALLOY TI-6AL-4V AT
ELEVATED TEMPERATURE**

THESIS

Onder Sahan, Lieutenant, TUAF

AFIT/GAE/ENY/02-11

**DEPARTMENT OF THE AIR FORCE
AIR UNIVERSITY**

AIR FORCE INSTITUTE OF TECHNOLOGY

Wright-Patterson Air Force Base, Ohio

Report Documentation Page

Report Date	Report Type	Dates Covered (from... to)
26 Mar 02	Final	Sep 2000 - Mar 2002

Title and Subtitle Fretting Fatigue Behavior of a Titanium Alloy Ti-6Ai-4V at Elevated Temperature	**Contract Number**
	Grant Number
	Program Element Number
Author(s) Lt Onder Sahan, TUAF	**Project Number**
	Task Number
	Work Unit Number
Performing Organization Name(s) and Address(es) Air Force Institute of Technology Graduate School of Engineering and Management (AFIT/EN) 2950 P Street WPAFB, OH 45433-7765	**Performing Organization Report Number** AFIT/GAE/ENY/02-11
Sponsoring/Monitoring Agency Name(s) and Address(es) Dr. Jeffrey Calcaterra 2230 Tenth St, Suite 1 WPAFB, OH 45433-7817	**Sponsor/Monitor's Acronym(s)**
	Sponsor/Monitor's Report Number(s)

Distribution/Availability Statement
Approved for public release, distribution unlimited

Supplementary Notes
The original document contains color images.

Abstract
The Purpose of this research is to investigate the fretting fatigue behavior of the titanium alloy Ti-6Al-4V at elevated temperature is investigated. Fretting and plain fatigue experiments are conducted at 260 . Crack initiation location and crack initiation orientation is measured and fretting and plain fatigue life data of the specimens from these tests are obtained. Fatigue parameters capable of predicting the number of cycles to specimen failure, the crack location and the crack orientation along the contact surface are analyzed. The parameters are calculated by using the computed stresses and strains obtained from the finite element analysis. The mechanisms responsible for the fretting fatigue crack initiation are determined. The effect of elevated temperature is examined by comparing room and elevated temperature fretting and plain fatigue data.

Subject Terms
High Cycle Fatigue, Fretting Fatigue, Elevated Temperature, Ti-6Al-4V, Predictive Parameters

Report Classification	Classification of this page
unclassified	unclassified
Classification of Abstract	**Limitation of Abstract**
unclassified	UU
Number of Pages	
116	

The views expressed in this thesis are those of the author and do not reflect the official policy or position of the Department of Defense, the US Government, or the Government of Turkish Republic.

AFIT/GAE/ENY/02-11

FRETTING FATIGUE BEHAVIOR OF A TITANIUM ALLOY

TI-6AL-4V AT ELEVATED TEMPERATURE

THESIS

Presented to the Faculty

Department of Systems and Engineering Management

Graduate School of Engineering and Management

Air Force Institute of Technology

Air University

Air Education and Training Command

In Partial Fulfillment of the Requirements for the

Degree of Master of Science in Aeronautical Engineering

Sahan Onder, B.S.

Lieutenant, TUAF

March 2002

FRETTING FATIGUE BEHAVIOR OF A TITANIUM ALLOY

TI-6AL-4V AT ELEVATED TEMPERATURE

Sahan Onder, B.S.

Lieutenant, TUAF

Approved:

_____/s/_____   _____

   Prof. Shankar Mall   (Chairman)   date

_____**/s/**_____   _____

   Prof. V. K. Jain   (Member)   date

_____/s/_____   _____

   Robert A. Canfield , Lt Col, USAF (Member)   date

Acknowledgements

Table of Contents

List of Figures

List of Tables

Abstract

Fretting fatigue crack initiation in titanium alloy, Ti-6Al-4V, at elevated

temperature is investigated experimentally and analytically using finite element analysis.

The temperature of this study is chosen to be 260 $°C$. Several specimens are tested at

different stress levels to establish the life data (i.e. S-N relationship). The crack initiation

location and the crack angle orientation along the contact surface are determined using

scanning electron microscopy. Finite element analysis is used to obtain the stress states

for the experimental conditions used during the fretting fatigue tests. These are then used

to investigate several critical plane based multi-axial fatigue parameters. These

parameters are evaluated based on their ability to predict the crack initiation location,

crack orientation angle along the contact surface, and the number of cycles to fretting

fatigue crack initiation. These predictions are compared with their experimental

counterparts to characterize the role of normal and shear stresses on fretting fatigue crack

initiation at elevated temperature. Also, plain and fretting fatigue data at room and

elevated temperature are compared. From these comparisons, it can be concluded that

260 $°C$ temperature does not have any detrimental effect on fretting fatigue crack

initiation of Ti-6Al-4V when compared to that at room temperature. Further, fretting

fatigue crack initiation mechanism in the tested titanium alloy appears to be governed by

the shear stress on the critical plane. However, further work is needed to understand the

role of both shear and normal stresses on the critical plane at elevated temperatures.

NOMENCLATURE

a	Contact half-width
a_{EXP}	Experimentally observed contact half width
a_{FEA}	FEA predicted contact half width
A	Cross sectional area
b	Half of the specimen thickness
e	X coordinate shift of the stick zone
E	Modulus of elasticity
f	Coefficient of friction
G	Shear modulus
k	Radius of curvature
m	Material fitting parameter
N_f	Number of cycles to failure
p_0	Maximum normal pressure in contact zone
P	Normal load
q	The surface shear stress
Q	Tangential load
Q_{max}	Maximum tangential load
Q_{min}	Minimum tangential load
r	Pad radius
R	Axial stress ratio

R_τ	Shear stress ratio
u	Displacement
w	Specimen width
β	Dundar's parameter
δ	Slip in the x-direction
$\Delta\delta$	Slip range at the crack location
$\Delta\sigma_{axial}$	Change in the axial stress
υ	Poison's ratio
θ	Observed angle of orientation
σ	Standard deviation
σ_{axial}	Axial stress
$\sigma_{axial,max}$	Maximum axial stress
$\sigma_{axial,min}$	Minimum axial stress
σ_{xx}	Normal stress in the x direction
$\sigma_{xx,FEA}$	FEA predicted stress in the x-direction
τ	Shear stress in the x y plane
τ_{max}	Maximum shear stress on critical plane

FRETTING FATIGUE BEHAVIOR OF A TITANIUM ALLOY

TI-6AL-4V AT ELEVATED TEMPERATURE

I. Introduction

Fretting is due to the application of oscillating tangential forces to two clamped surfaces. When either or both of the contacting bodies are subjected to repeated loads that can cause the initiation and propagation of fatigue cracks, the system is said to experience fretting fatigue. The United States Air Force is interested in this phenomenon, because it is commonly encountered in gas turbine engines. Fretting fatigue becomes an important issue at the interface between the turbine engine disk slot and blade attachment (Figure 1.1). Further, these components are subjected to the high temperature. These conditions, therefore, leads to failure or to an increase in maintenance cost due to the reduced part life. For this reason, in order to prevent the unexpected failures or to reduce the maintenance cost, the fretting fatigue crack initiation mechanisms at elevated temperature must be identified. The purpose of this research is therefore to investigate the fretting fatigue crack initiation behavior of a titanium alloy, Ti-6Al-4V at elevated temperature. The reason of investigating this material is that it is commonly used in aircraft engine components.

One of the most damaging aspects of fretting is the large reductions in fatigue strength. Room temperature studies of a wide variety of alloys are abundant but to date there has been little published information on the fatigue behavior of materials at high temperatures in the presence of fretting. Those which has been reported generally

concerns practical attempts to reduce the effects of fretting fatigue at high temperatures and usually involves some form of surface treatment.

Fretting fatigue research is the study of the combined effects of fatigue and wear. In order to get these effects, in this study a simplified geometry and loading condition, which represent the very complex turbine engine geometry and loading conditions, is used. Figure 1.2 shows the simplified experimental configuration of this study. The two bodies of interest are the fretting fatigue specimen and the fretting fatigue pad, (Figure 1.3). These bodies are pressed together through the use of lateral springs, which apply a constant normal load, P. The servohydraulic test machine is used to impose the axial stress, σ_{axial}, on the fretting fatigue specimen. This introduces a tangential load, Q, which is dependent on the stiffness of the longitudinal springs. Note that in Figure 1.3, r is the radius of pad curvature, b is the specimen half thickness, A is the specimen area and 2a is the contact width.

In this study, in addition to the configuration that is explained above, two infrared spot heater lamps are focused on the contact region to achieve high temperature. K type thermocouples are used. The temperature of the experiments is chosen to be 260 $°C$. This temperature is the operating temperature of this material. The configuration of the experiment for each test is same but the applied loads are varied to obtain fretting fatigue crack initiation in both the low and high cycle fatigue regimes. Furthermore, plain fatigue experiments at elevated temperature are performed in order to have a complete fretting fatigue data.

The studies until now considered the fretting fatigue at room temperature. However, the main objective of this research is to investigate the temperature effect on

fretting fatigue of a titanium Ti-6Al-4V. In this study fretting fatigue life curve at elevated temperature is obtained and also crack initiation prediction analysis is made. Further, several fatigue parameters are considered. The quantities, such as stress, strain and displacement that are used to develop the fatigue parameters, are determined by finite element analysis. An emphasis is placed on developing these fatigue parameters near the stress concentration. Figure 1.4 shows typical fretting fatigue stress concentration in the x-direction.

The fretting fatigue crack initiation parameters are evaluated on their ability to predict the experimental observations, and the mechanisms responsible for the fretting fatigue crack initiation are also determined. The experimental observations are the number of cycles to crack initiation, the crack location and the crack orientation along the contact surface. For this purpose, the fretting fatigue specimens are examined to determine the crack location and the crack orientation along the contact surface. Finally, the effect of temperature is examined by comparing both fretting and plain fatigue data at room and elevated temperatures.
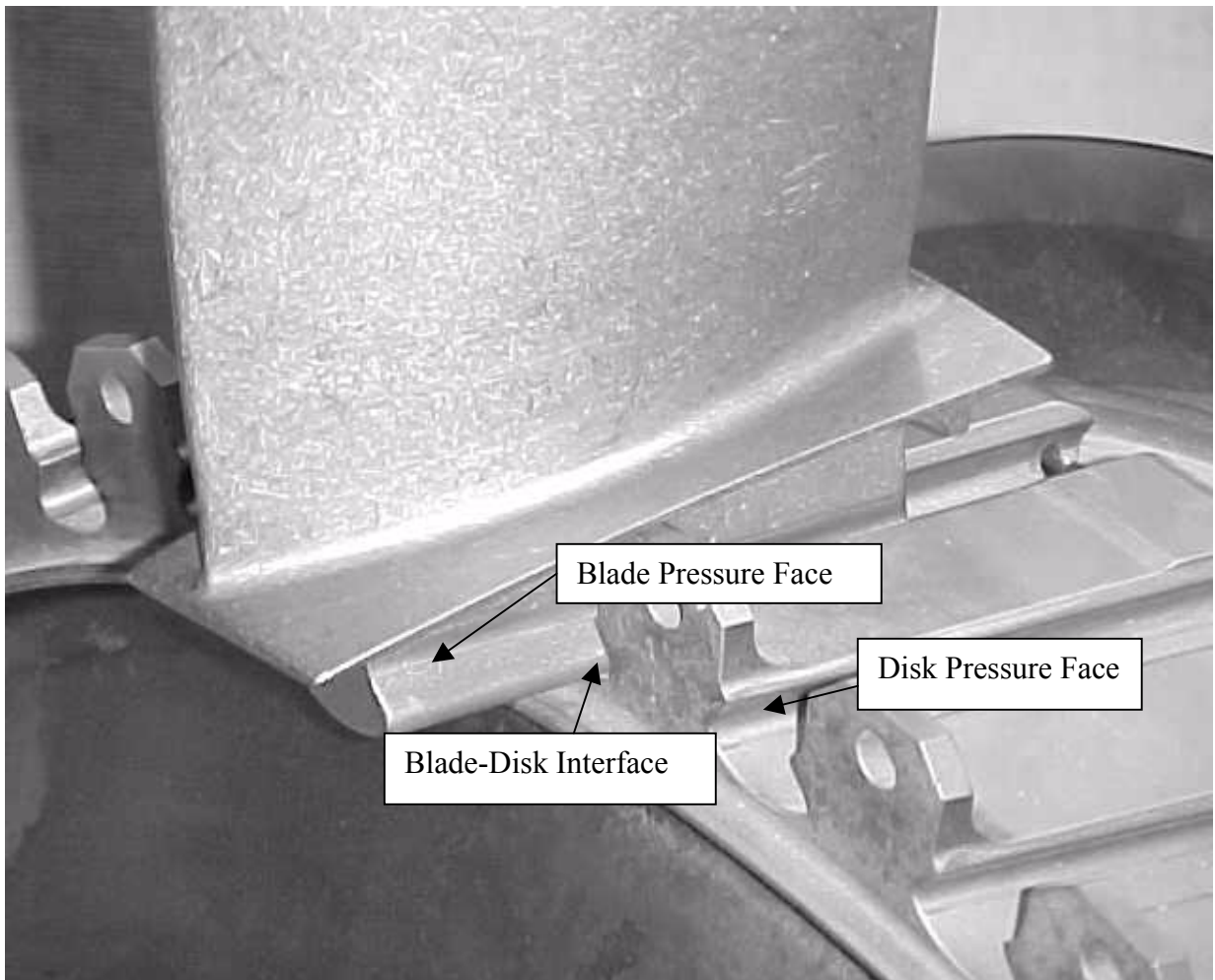
Figure 1.1. Turbine Engine Blade-Disk Interface.
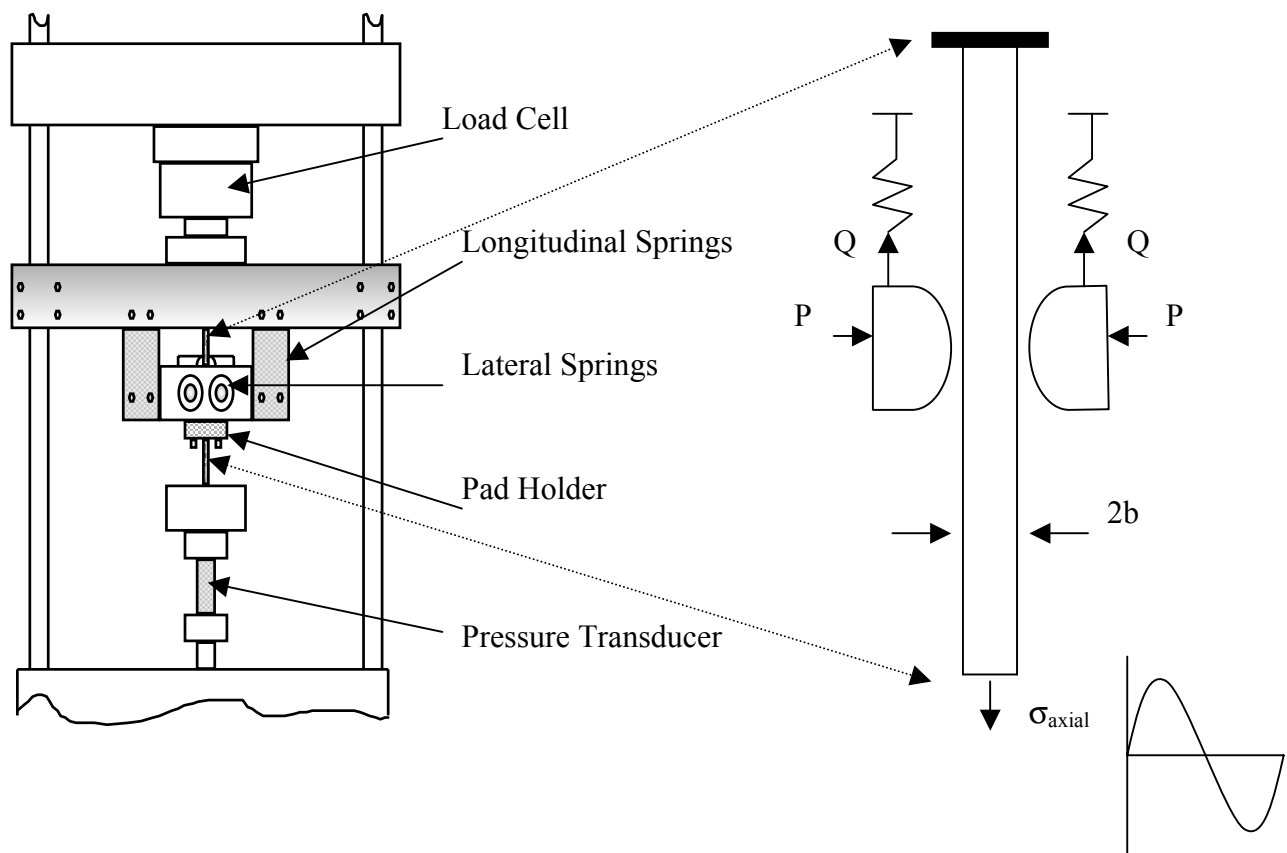
Figure 1.2. Fretting Fatigue Experimental Setup.

r

P

Body 1-Pad

Q

Body 2-Specimen

$A\sigma_{axial} - Q$

2a

x

b

$A\sigma_{axial}$

Line of Symmetry
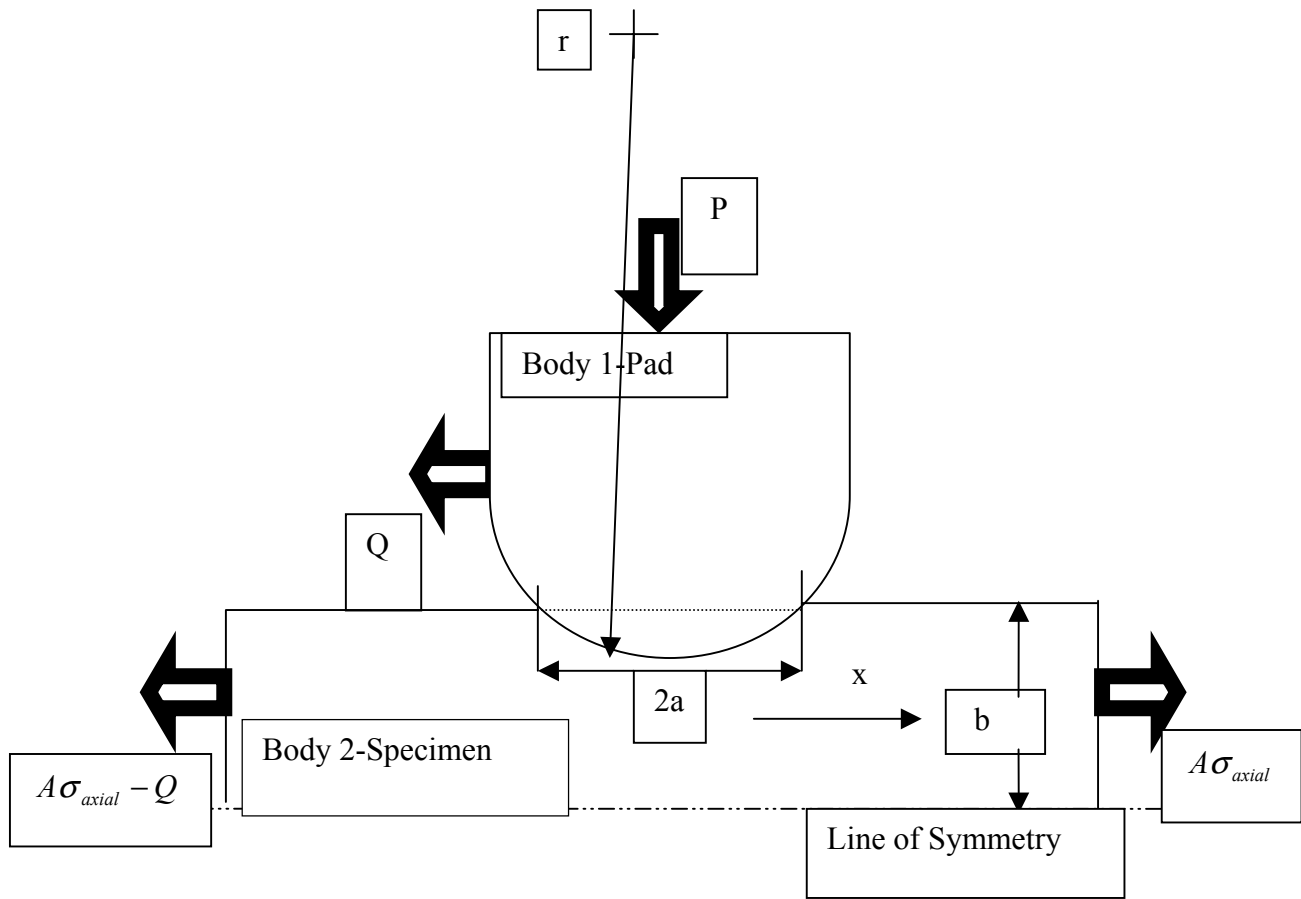
Figure 1.3. Free Body Diagram of Two Bodies Under Fretting Fatigue Loading.
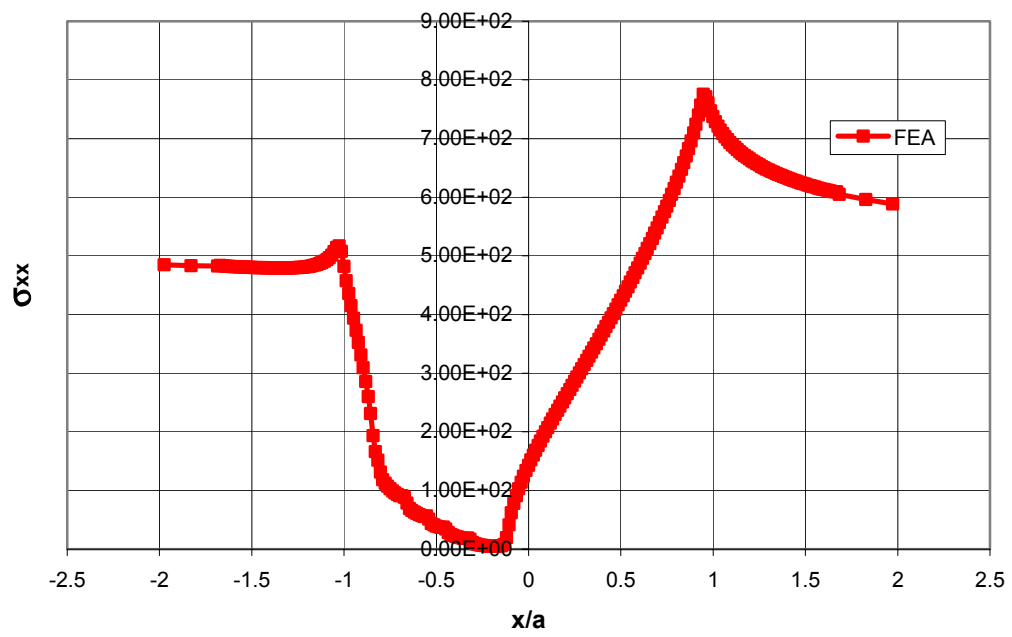
Figure 1.4. Normal Stress Concentration.

II. Background

In this chapter, first the work that has been accomplished in the fretting fatigue history and parameters is mentioned. And the second topic of this chapter is high temperature studies in this area. Finally fretting contact analysis is explained.

Summary of Fretting Fatigue Research

It is very well known that the first identification of fretting fatigue came from Eden, who noted the formation of iron oxide on the surface of a fatigue specimen in the areas contacting the grips of a test machine, in the early part of this century at 1911, as stated by Birch [1]. He also notes that the phenomenon of fretting was referred to as friction oxidation, wear oxidation, false brinelling, bleeding, and 'cocoa' in 1950s.

While US military was getting concerned over fretting fatigue in 1960s, the real application of the scientific investigation of fretting fatigue to engineering practice commenced around 1965 with the development of the concept of a life reduction factor for fretting. And also the study of very well-known fretting researchers Nishioka, and Hirakawa [2] emerged in 1968-69. They addressed several critical fretting fatigue issues, and proposed a model for predicting fatigue life under fretting conditions that was a function of slip amplitude, contact pressure, and materials. They also observed that the cracks initiate at the edge of contact and propagate at an angle to the surface of the specimen, which is shown in this study too.

Many developments in understanding the mechanisms of fretting fatigue occurred during the 1970s and 80s. A NATO conference, as stated in Birch's study, on fretting

fatigue in aircraft components in 1974 "added to the existing impetus to perform research".

The following paragraphs will explain in a historical way what has been done from 1985 to 2001 concerning fretting fatigue. Some authors considered what palliative effects can be achieved for fretting fatigue by modifying the contact conditions. One of those authors is Chivers [3] who found that fretting fatigue is the result of such tensile stresses contributing to the crack initiation process. He examined the effect on these tensile stresses for modifying the contact conditions of the friction coefficient and clamping force, so that successful palliatives can be identified. The analysis showed that conditions exist where increasing or decreasing either the friction coefficient or clamping force can be of benefit, and there is no panacea. However his analysis provides an explanation of the apparent contradictions in the literature, and he makes suggestions for the best approach to ameliorate a fretting fatigue problem, given this complicated situation.

While some authors were dealing with the idea of how to ameliorate the fretting fatigue problem, Broszeit [4] studied a new method of experimentation. He studied the fretting fatigue behavior of the alloy Ti-6Al-4V with the aid of a model apparatus. The approach employed in the study was based on the fretting fixture test principle, which was similar to the one that is used in this study. Attention was given to the fretting fixture arrangement, typical damage observed in the case of a specimen fractured in a fretting fatigue test, and the significance of the stress distribution in the system of specimen and fretting fixture. The investigation of the stress and slip distribution in the contact system specimen-fretting fixture was discussed, taking into account the finite element structure

and stress distribution, the stress profile in the contact area of specimen and fretting

fixture during a cycle of load, the distribution of slip between specimen and fretting

fixture, and the material stressing in the contact area.

In 1987 a new fretting fatigue test device was designed and built for special

fretting fatigue studies with composite materials by Friedrich [5]. The device was

attached to the specimen grips of a servohydraulic testing machine and allows

symmetrical fretting loading of the specimen surface by two fretting pads while the

specimen was fatigued. Positioning of the fretting pads could be either on the edges of

laminated samples or on their flat surfaces. Different fretting slip amplitudes could be

specified at given fatigue conditions, and the fretting load could be exactly adjusted and

controlled.

In the same year Li [6] from China made some series of experiments and found

that the fretting fatigue limits for 0.45 C steel and high-strength aluminum alloy

specimens have been reduced by 30-55 percent compared to nonfretted specimens at 10

million cycles. In the most severe case, fatigue strength was reduced by about 80 percent.

Laboratory tests on aircraft components have shown that about 90 percent of all failures

occur at points where fretting occurs.

In the mean time another paper by Sakata [7] from Japan presented an application

of fracture mechanics to fretting fatigue analysis. This analysis utilized the stress

intensity factors calculated from the stress distributions at the tip of cracks growing from

the contact edges. These stress distributions were themselves analyzed using the

boundary element method program that was specially developed for these types of

contact problems. The fretting fatigue limits were estimated by comparing the above

mentioned calculated results of stress intensity factor ranges with the threshold stress intensity factor ranges of the material itself. Also estimated was the influence of the mean stress on the fretting fatigue limit. The author stated that good agreement existed between the calculated results obtained and the previous experimental results from fretting fatigue tests.

Another paper from Japan by Hattori [8] in the next year proposed an estimation method for fretting fatigue strength. He analyzed the characteristics of fretting fatigue cracks using stress intensity factors at the tip of cracks growing from the contact edges. The stress intensity factors were calculated from the contact pressure and tangential stress distributions on the contact surfaces. Fretting fatigue limits were estimated by comparing the stress intensity factor ranges with the threshold stress intensity factor range of the material. These calculated results were then compared with experimental results of fretting fatigue tests.

Mingjian [9] found a way to predict distribution of fretting damage along the interface and crack location. He designed a dovetail joint specimen to model a blade-to-disk joint in a typical gas turbine. The method made it possible to determine the stress and temperature fields in the contact surface and the nearby area, to estimate the state in interface (stick, slip, or separation), and to know how much energy is consumed for friction in the contact surface. Two years later Mingjian [10] also discussed the feature of fretting fatigue and stress distribution of a blade-to-disk circumferential dovetail joint in a typical gas turbine. He presented a method to determine the fretting extent and to predict the fretting fatigue life.

11

Abidnazari [11,12] published some papers on fretting fatigue in the 90s. The results obtained and presented in his papers illustrated the existence of a normal pressure threshold (the value after which increasing the pressure does not affect the life) in fretting fatigue. This finding has led the authors to question the role of normal pressure and frictional stress in fretting fatigue failure. He explained that this was because at a given applied cyclic stress and below the pressure threshold, fretting fatigue failure was a function of normal pressure and the change in normal pressure, hence by the first law of friction: fretting fatigue failure was a function of frictional stress and the change of frictional stress. Above the pressure threshold, fretting fatigue failure was just a function of normal pressure and frictional stress, not the increase of these two variables. In conjunction with these findings, it has been argued that a critical frictional stress might exist that causes the fretting damage to reach its threshold faster.

Szolwinski and Farris [13] placed a particular emphasis on the effect of the subsurface stress field that is associated with three-dimensional fretting contacts on fretting fatigue crack initiation and propagation. The calculation relied on recent closed-form expressions for the subsurface stress field induced by circular stick/slip regions of contact. Assuming fatigue crack initiation was controlled by the effective stress in the von Mises yield criteria allowed the effect of normal and tangential loads and the coefficient of friction on fatigue crack initiation to be predicted. It was shown that the effect of friction of the subsurface maximum shear of the classical Hertzian contact was slight. However, the coefficient of friction and tangential load had strong effect on the tensile stress at the edge of contact. These tensile stresses were consistent with fretting

fatigue cracks that lead to the multi-site damage of primary concern to the aging aircraft problem.

In Hoepner's [14] report that contains a review of the literature pertinent to fretting and fretting fatigue including special applications to aircraft joints, he indicates there are three stages to fretting fatigue life. The first is a period of crack nucleation, usually accompanied by adhesion and plastic deformation of contacting asperities in relative motion. In the second stage, propagation of nucleated cracks is determined by the stress resulting from the surface tractions imposed by fretting. The results of several investigations of the stress state and its effect on the propagation of nucleated cracks are discussed. The stress state can either dramatically increase early crack propagation rates or retard crack propagation, depending upon the specifics of the contact under study. The third stage is a period of crack propagation during which fretting contact stresses are not significant to crack propagation.

Switek [15] performed some series of experiments that are similar to what we will do in our research. The experimental considerations presented in this paper refer to flat specimens, with a special bridge clamped to their surfaces, subjected to axial cyclic loading, transversal clamping load, and a friction force appearing on contacting surfaces. His theoretical analysis showed that the highest tensile stress exists at the edge of the bridge along with the maximum level of an elastic strain energy. The fatigue experiments and the metallographic examinations of the specimens proved the theoretical assumption that the fatigue crack propagates in such a direction, that the total strain energy decreases. The main crack, which is responsible for the final fracture of the specimen, originates from the edge of the bridge, propagates initially at a 45 deg angle to the surface and,

while growing, gradually becomes perpendicular to the surface. His paper also presents a theoretical approach to the conditions of development of short fatigue cracks remaining in the area of residual stresses appearing as the result of clamping pressure.

Similar experimental research accomplished by Szolwinski [16] revealed that the critical location for crack formation is the trailing edge of contact, consistent with observations that he made in the laboratory.

Meanwhile Hattori [17] used the stress singularity parameters at contact edges to estimate the initiation of fretting fatigue crack. The propagation behavior of this fretting fatigue crack was estimated using fracture mechanics analysis. Also he stated in his paper that fretting fatigue cracks initiate very early in fretting fatigue life, and fretting fatigue life is dominated by the propagation process of small cracks. Thus, the prediction of fretting fatigue crack initiation and crack propagation behavior is very important for estimating fretting fatigue strength.

One recent study performed by Iyer et al [18] showed that increasing the contact pressure reduces life at 1 Hz but does not have any effect at 200 Hz. The constant-amplitude tests had been performed at cyclic frequencies of 1 and 200 Hz. Two values of contact pressure were considered. The cyclic frequency of 200 Hz was found to curtail the constant-amplitude fretting fatigue life regardless of the contact pressure applied.

The parameters that govern the life of metallic materials under conditions of fretting fatigue may be divided into two broad categories. The first category deals with the material properties and characteristics (e.g., yield strength, elastic modulus, surface roughness, etc.) while the second includes the externally imposed loading conditions and contact geometry. The two materials in contact may either stick, slip, or stick-slip (i.e.,

14

there is a slip and a stick region within the contact interface) with each other. It has been shown by Iyer et al [18] that the life reduction is highest under partial slip.

Lykins [19] separated the work accomplished in the parameters area by four distinctive techniques, as empirical techniques, fracture mechanics techniques, plain fatigue techniques, and finally fretting fatigue specific techniques. He mentioned in his paper that in each of the empirical studies he reviewed, intent was to establish the fact that fretting fatigue reduces the plain fatigue strength due to parametric variations of certain applied loading conditions, specifically the applied normal pressure. However, he stated that no attempt was made to determine the relationship between the change in applied loading condition and the change in the stress or strain along the contact surface.

He discouraged the use of fracture mechanics technique, because an initial crack length had to be assumed, and it was impossible to know exactly the amount of life consumed to reach the initial crack length. Furthermore, the fracture mechanic technique assumed the crack orientation in order to conduct the analysis.

When Lykins talked about fretting fatigue specific techniques he mentioned Ruiz [20] who proposed the κ_2 parameter. This parameter gives a good idea of the possible fretting fatigue crack initiation location. It combines the effects of the surface tangential stress, the surface shear stress, and the relative slip at the interface. This parameter can be written as

$$\kappa_2 = (\sigma_T \tau \delta)_{max} \tag{1}$$

Ruiz also proposed a parameter that combines the maximum tangential stress with the maximum frictional work, as in

$$\kappa_1 = (\sigma_T)_{max} (\tau \delta)_{max} \tag{2}$$

These parameters combined several fretting fatigue crack initiation parameters into one criterion which explains that the frictional work term in these equations represents the mechanism that nucleates cracks while the maximum tangential stress represents the mechanism that opens and propagates the nucleated cracks.

Interest in fretting fatigue continues, as the problem has not been solved by any estimation. And our interest is the temperature effect on fretting fatigue. In the following pages the work that has been done in this area is explained.

High Temperature Studies

Several studies on the elevated temperature fretting fatigue behavior of various materials clearly indicate the life debit due to high temperature. However, they mainly focus on different objectives other than the objectives that are presented in this study. Now some of these studies and their main objectives are mentioned in the following.

Waterhouse [21] conducted research on metallurgical changes in the high temperature fretting of Ni and Ti alloys in 1977. He used Ti-6Al-4V specimens which were subjected to fretting fatigue at $200, 400, 600\ °C$. He examined layer formation on each specimen in scanning electron microscope (SEM). SEM examination of fretted surfaces showed that layered structures developed at $200\ °C$ and these were more marked at $600\ °C$ developing into elephant trunk growths.

Another author who worked with titanium alloys was Elder [22]. He studied surface property improvement in titanium alloy gas turbine components through ion implantation. Detailed/microscopy and mechanical test results were used to analyze the

various mechanisms contributing to wear and fretting fatigue damage in titanium alloys at room and elevated temperatures.

In the same year Mutoh [23] carried out a series of fatigue and fretting fatigue tests of two steam turbine steels at room temperature and 773 °K. He showed that the values of the friction coefficient at 773 °K was almost equal to those at room temperature, and the reduction of fatigue life and strength in the fretting test were significant at both temperatures.

The high sensitivity of titanium alloys to fretting fatigue has to be taken into account when oscillatory relative motion occurs in joints of fatigue loaded components, e.g., in the connection of the disc with the blades in compressors of aircraft engines. For this reason another paper on fretting fatigue strength of Ti-6Al-4V at room and elevated temperatures came from Germany by Schaefer [24]. He investigated fretting fatigue behavior of Ti-6Al-4V at room temperature and service temperature ($350\ °C$) as well by testing flat specimens under fatigue loading and simultaneous fretting applied by a special fretting apparatus. He found that elevated temperature ($350\ °C$) had little detrimental effect.

Waterhouse [25] published another paper on fretting wear and fretting fatigue at temperatures up to $600\ °C$. He found that raising the temperature increased the oxidation rate of most alloys. The thicker oxide film prevents metal-to-metal contact and reduces the coefficient of friction. Both high temperature and sliding were necessary for its formation. The result was that the wear is much reduced and also fatigue strengths are increased. It was only stable at the high temperature. When the temperature fell to room temperature it was soon completely disrupted. The evidence was that the alloys which

were capable of forming the glaze oxide were those on which an oxide with a spinel structure could develop. Titanium alloys did not develop this type of oxide.

Finally Dai [26] studied several effects on plain fatigue life (PFL) and fretting fatigue life (FFL). He carried out the effects of contact pressure, amplitudes, applied loads, temperature, number of cycles, and the high-cycle to low-cycle load ratio on fretting fatigue life and frictional coefficient. The test results indicated that with the increasing temperature the FFL decreased from room temperature to 200 $°C$, increased at about 300 $°C$, and decreased again. SEM studies revealed that it was flake-like oxide that protects the contact surface from further damage and results in an enhancement of the FFL.

Review of Fretting Contact Mechanics

As described by Hills and Nowell [27], two kinds of contact conditions can be of the concern here. These are a complete or an incomplete contact geometry conditions. Complete contact produces a contact area that is independent of load, as with a flat punch on a plane. Incomplete contact, e.g. the cylinder on a flat plate, produces a contact area whose size depends on the magnitude of the normal force. Although contact area is variable for incomplete contact, the contact pressure is at all places non-singular, falling continuously to zero at the edge of contact. A complete contact condition necessarily has singularities at its outside edges that are accommodated by local plasticity, and are thus more difficult to model analytically or numerically than nonsingular cases.

After this brief description of contact types, the analytical solution to the total stress in the x-direction along the contact surface of the contacting bodies as result of the

normal, the tangential and the axial load is discussed next. The relationships in the

contact region can be defined as follows:

$$\frac{1}{A^*}\frac{\delta h}{\delta x} = \frac{1}{\pi}\int\frac{P(\xi)}{x-\xi} - \beta q(x) \tag{3}$$

where h(x)=$v_1(x) - v_2(x)$, is the amount of overlap that would occur if the

contacting bodies could freely penetrate each other, p is the pressure in the contact zone

and q is the surface shear stress. The other parameters of equation (3) are

$$A^* = 2\left\{\frac{1-v_1^2}{E_1} + \frac{1-v_2^2}{E_2}\right\} \tag{4}$$

which is the composite compliance and Dundar's parameter is given as follows

$$\beta = \frac{1}{2A^*}\left\{\frac{1-2v_1}{E_1} - \frac{1-2v_2}{E_2}\right\} \tag{5}$$

where E and v are modulus of elasticity and Poisson's ratio for the respective bodies. A

similar equation can be formulated, if we assume the tangential displacement to be

defined by g(x)=$u_1(x) - u_2(x)$. The resulting equation is as follows

$$\frac{1}{A^*}\frac{\delta g}{\delta x} = \frac{1}{\pi}\int\frac{q(\xi)d\xi}{x-\xi} + \beta p(x) \tag{6}$$

where $u_1(x)$ and $u_2(x)$ are the displacements in the x-direction.

Equation (3) and (6) can be simplified, because the contacting bodies in this thesis

are made of the same material and therefore $\beta = 0$.

The solution of the pressure resulting from the normal load is usually termed the

Hertz solution. The Hertz solution can be visualized by bringing the fretting pad into

contact with the fretting fatigue specimen with a normal load. This leads to two possible

assumptions about the contact dimension and the contact relationship between the two

19

bodies to solve for the ensuing pressure distribution. These assumptions are that the radii of both bodies are large in comparison to the contact dimension and that the contacting bodies have infinite boundaries. This infinite boundary is commonly referred to as a half space.

In order to be able to make a half space assumption b, one half of the specimen thickness must be at least ten times the contact half width, a, or b/a >10. However, the violation of the infinite boundary assumption will cause a deviation from the analytical solutions, because Fellows et al. [28] found that for the final dimensions, i.e. b/a = 3 in their study, had a significant effect on the surface stress in the x-direction. In addition to half space assumption, it can be also assumed that the local profile of contact surfaces can be idealized as a parabola. This leads to the following weight function

$$w(x) = \sqrt{a^2 - x^2} \tag{7}$$

where, a, is the length of contact. By using equation (7) and (6) the pressure distribution can be defined as

$$p(x) = -p_0 \sqrt{1 - (x/a)^2} \tag{8}$$

the resulting maximum pressure is given by

$$p_0 = \frac{2P}{\pi a} \tag{9}$$

here P is the applied normal load. The stress in the x-direction at the contact interface, resulting from the normal load or equation (8), can be expressed in Cartesian coordinates as follows

$$(\sigma_{xx})_{normal} = -p_0 \frac{\sqrt{a^2 - x^2}}{a} \tag{10}$$

The analytical solution of two cylindrical bodies in contact is described by Hills and Nowell [27], where both a normal load and a tangential load are applied, and the resulting equation of the stress distribution in the x-direction as of the tangential load can be expressed as follows

$$(\sigma_{xx})_{\tan gential} = 2fp_0 - \frac{2}{\pi}\int_{-a}^{a}\frac{q'(x)}{x+a}dx \qquad (11)$$

where

$$q'(x) = -f \cdot p_0 \frac{c}{a}\sqrt{1-((x-e)/c)^2} \qquad (12)$$

and e is the x coordinate shift of the stick zone, which can be formulated as

$$e = b = \frac{\sigma a}{4fp_0} \qquad (13)$$

Also, c is the stick zone boundary and can be defined as

$$c/a = \sqrt{1-|Q/fP|} \qquad (14)$$

here Q is the reacted tangential load and f is the coefficient of friction.

Finally, the total stress in the x-direction along the contact surface of the fretting fatigue pad and fretting fatigue specimen can be expressed as the sum of the normal load, the tangential load and the axial load, which can be written as follows

$$\sigma_{xx} = (\sigma_{xx})_{normal} + (\sigma_{xx})_{tengential} + (\sigma_{xx})_{axial} \qquad (15)$$

Since the thickness of the fretting fatigue specimen is less than ten times b/a in this study, it is necessary to make a finite element analysis. Later, these finite element results are used to determine the governing parameters along the contact surface, such as stress, strain and displacement. In order to validate the results of finite element method an alternative numerical technique is used in this study. Chan and Lee [29] have written a

21

Fortran program to carry out the numerical analysis required for the solution of equation

(15). The results from their program and the results from finite element method (FEM)

are compared in Chapter IV to validate the results of FEM and these values are

eventually used to develop the fatigue parameters for fretting fatigue crack initiation at

elevated temperature.

III. Experimental Studies

In this chapter, experimental setup and results are presented. First of all, fretting fatigue experimental configuration at elevated temperature is discussed. As studies related to the elevated temperature are of concern here, controlling the elevated temperature at this configuration is explained. Coefficient of friction studies, determination of loads, crack location and crack orientation along the contact surface are the other topics of this chapter. Also, a comparison between room and elevated temperature data for both plain and fretting fatigue is made.

Fretting Fatigue Experimental Configuration at Elevated Temperature

In this study, a rigidly mounted fretting fixture was used, which was attached to a 22.2 kN servohydraulic load frame (Figure 1.2). Fretting fixture is capable of keeping the normal load constant via lateral springs throughout the test. The tangential load in this study was a function of the axial load and the stiffness of the longitudinal springs used to mount the fretting pads. A typical tangential load profile versus cycles for this test configuration is shown at Figure 3.1. Note here that $\frac{Q_{min}}{Q_{max}}$ ratio for this test configuration is approximately between -0.3 and -0.4. Further, the axial load can be varied with the help of the 22.2 kN servohydraulic load frame. Load cells were attached to the servohydraulic load train in order to control and monitor the axial load variation that the test specimen experiences during the fretting fatigue test. When a cyclic load is applied on the specimen, the contact pads move relative to the specimen and cause a fretting

23

action on the specimen surface. That's why alignment becomes a big concern here. For this reason the alignment is checked before the series of tests starts and is also checked all the time before each test during the course of this study. The 22.2 kN servohydraulic load frame, the fretting and heating lamps fixture are shown in Figure 3.2 together.

Constant amplitude fretting fatigue tests are conducted at 10 Hz, over a wide range of axial stress conditions, σ_{max}=350 MPa to 600 MPa , and the axial stress ratio is chosen to be R = 0.1. The control system of the test equipment maintains the frequency and the amplitude of the applied stress constant during the test duration. The dimensional and material properties of the fretting fatigue specimen are as follows: specimen thickness, 2b = 3.86 mm, specimen width, w = 6.35 mm, cross sectional area, A = 24.511 mm^2. The cylindrical pads that are used has the radius of r = 50.8 mm. The specimen and the pads are shown in Figure 3.3. The fretting fatigue specimen and pad material are made from a titanium alloy Ti-6Al-4V. The reason of choosing this material is that because it is widely used to fabricate turbine disks and blades. The modulus of elasticity, E, of Ti-6Al-4V at 260 $°C$ is determined to be 95 GPa.

The temperature is measured and controlled using a calibrated Type K thermocouple attached on the pad surface which is in contact with the specimen surface at the center of the gauge length (Figure 3.4). The reason for using pad surface temperature as feedback temperature is that because failure occurred at the point when thermocouple was attached on the specimen. Welding of thermocouples to the specimen creates some kind of damage on the specimen surface, and this damage causes the specimen to fail at a very early stage of cycling. For this reason, the indirect method is used to control the temperature during the fretting fatigue tests.

The temperature of the pads is calibrated, and it is found that to get 260 $°C$ on the specimen, 250 $°C$ on the pads has to be reached. The temperature on the pads is monitored during the tests. A typical temperature profile is shown at Figure 3.5 for this test configuration. Note here that the temperature is kept constant within ± 3 $°C$ during the tests. The specimens are kept at the test temperature at least 2 hours before starting the tests.

Two infrared spot heater lambs are used to achieve the test temperature. The schematic diagram of the test set-up (Figure 3.6) shows the fretting fatigue specimen, the contact pad, and the two lamps placed at the front and at the back of the specimen. In addition, the spot heaters that are used in this study are shown in Figure 3.2. The lamps of these heaters heat up and cool down instantly in response to power control signals. They reach 90 % of full operating temperature within three seconds of a cold start. The infrared energy emitted from these heaters can be adjusted to match the heating requirements of a variety of applications. A reflector shield is used with the spot heater to contain the infrared energy within the desired target area. The reflector directs the infrared energy supplied by a tubular quartz, infrared lamp to a spot at the ellipse focal point [33]. For this reason, focusing the lambs is very important concern. In order to achieve a good focusing, calibration tests are conducted. The configuration of this spot heater is shown in Figure 3.7.

The signal for feedback temperature is calibrated at elevated temperature using a "dummy" specimen, having the same geometry as the real specimens. During calibration, the temperature is controlled at six different locations along the specimen. These studies are done to achieve an acceptable temperature profile along the specimen. The

temperature profile is shown in Figure 3.8. The motivation here is to keep the temperature constant at contact region and also in its nearby region. Note here that at the center of the specimen, which is the contact area of the specimen and the pads, the temperature profile can be considered constant.

The plain fatigue experiments of this study are done with the same 22.2 kN servohydraulic load frame, however the fretting pads are removed, and the temperature studies are redone. For this configuration, instead of using indirect method, direct method is used. During temperature studies of these experiments, some problems are encountered, and these problems are mentioned in Appendix A. In order to attach the thermocouples on the specimen high temperature epoxy glue is used at these experiments, and to achieve the test temperature same spot heaters are used. With this type of configuration three tests are done, which are presented at the later part of this chapter.

Coefficient of Friction Studies

In order to perform the finite element analysis (FEA), which is the main objective of Chapter IV, the coefficient of friction has to be determined so that it can be used as an input data in FEA. For this reason, some experiments are carried out for the determination of the coefficient of friction. In these experiments, the tests are done in displacement control. The axial load increases until it becomes constant. This load value is then considered to be equal to the friction force or limiting sliding force on the specimen, and by using the normal load value of the test the coefficient of friction is determined.

Previous studies [18,19] showed that after cycling the specimen, the coefficient of friction increases. For this reason, the determination of coefficient of friction is done after cycling the specimen until it reaches a constant value. In this study, it is determined first without cycling the specimen, and then it is determined after 5000 cycles and 10000 cycles at elevated temperature. It is observed that at 10000 cycles, the coefficient of friction reaches to a constant value. The results of this study are shown in Figure 3.8. From this figure, the coefficient of friction that is used in finite element analysis is chosen to be 0.55.

Load Determination

In this study, the axial load and the tangential load has to be determined so that these loads can be used in the finite element analyses as the input conditions. The axial load is monitored by the load cells that are attached to the 22.2 kN force frame and actuator during the experiments.

The tangential load is a function of both axial load and normal load. By using the data from actuator and frame load cells reading, the tangential load can be found by the following formula

$$Q = \frac{F_A - F_F}{2} \tag{16}$$

here Q is the tangential force, the others represent the force reading of actuator and frame. The reason for dividing by 2 is that there are two pads that are in contact with the specimen. As mentioned before, Figure 3.1 shows the typical $\frac{Q_{min}}{Q_{max}}$ ratio for this test configuration.

The normal load is applied with the aid of two lateral springs (Figure 1.2). The load is held constant for the duration of the test and is monitored with two load cells. The normal load is chosen to keep the maximum stress in the x-direction of the specimen below the yield stress. A normal load, P=1.33 kN is used in all tests.

The experimental fretting fatigue data for the tests at elevated temperature is summarized on Table 3.1. This summary of the experimental data provides: specimen number, the axial stress change, $\Delta\sigma_{axial}$, total number of cycles to rupture, N_f, the maximum axial stress, $\sigma_{axial,\max}$, the minimum axial stress, $\sigma_{axial,\min}$, the maximum tangential load, $Q_{\max}$, and the minimum tangential load, $Q_{\min}$. It should be noted that the maximum number of cycles, that a test is subjected to, is 4×10^6 cycles.

Crack Location

In this part, the experimentally observed crack location is discussed. The predicted crack location should correlate with the observed crack location. This comparison of the predicted and observed crack location is given in Chapter IV.

Previous studies [18,19] show that the crack location occurs near the trailing edge of contact or near x/a = 1.0. The trailing edge is the region where the stress concentration in the x-direction is a maximum (Figure 1.5). However it is known that it is difficult to determine the precise crack location, because the specimen is tested up to rupture. Some authors [19] showed that at specimen failure or at the drop in the load cell output, the specimen compliance changes as a result of the increasing crack size. The increasing crack size exposes more of the specimen surface to the path surface, which results in larger contact widths than those that are predicted from the finite element method.

Also some studies have demonstrated the good agreement between the predicted contact width from the finite element analysis and the observed value. In order to show this agreement the fretting fatigue test is stopped when there is drop in the load cell reading. This study shows that the experimental 2a =0.994 mm while the predicted 2a is 0.944 mm. So this study indicates that the predicted crack location from finite element analysis can be used, because they are in good agreement. The crack location discussion of finite element analysis is presented in the following chapter.

To conclude, the crack location occurs near the trailing edge of contact or at x/a = 1.0, which also coincides with the approximate location of the computed location for the stress concentration in the x-direction.

Crack Orientation

Another important issue of this study is to find the crack orientation along the contact surface. The main motivation here is to find a relationship between the predicted angle of crack orientation and the observed angle of crack orientation, which then can be used to validate the suitability of the crack initiation parameter.

The procedure to get this angle is as follows: First of all failed specimen (Figure 3.10) is sectioned along the direction as shown in Figure 3.11. The sectioned specimen is mounted in a transparent medium, ground, and polished by hand to ensure that sectioned surface is at the center of the crack initiation zone. This crack initiation zone is found as the region with discoloration on the failed specimen surface as shown in Figure 3.11. The polished specimens are coated with gold in order to increase their conductivity and

placed in the scanning electron microscope (SEM) to evaluate the orientation of the crack along the contact interface.

There are two types of cracks that can be found in a fretting fatigue study. These are known as primary and secondary cracks. The first type of crack is the crack that leads to specimen rupture. The other type of crack does not lead to specimen rupture, but can be detectable by the SEM along the contact surface. Figure 3.12 shows the primary crack of specimen 5. Note that the experimentally observed angle of orientation, θ, along the contact surface is about $\theta = -45°$. However, there was no secondary crack for this specimen. For this part of the thesis, only two specimens are sectioned and analyzed, because the results are consistent with the ones that are predicted by analytical methods and the ones that are observed by other authors.

In conclusion, the sectioned specimens showed that the crack orientates at some angle to the axial stress direction along the contact surface, but at a certain depth of propagation, the crack orientates perpendicular to the axial stress direction.

Comparison: Elevated Temperature Versus Room Temperature Data

In this section, the fretting fatigue and plain fatigue data at elevated temperature and at room temperature are compared. The experimental data are compared based on the applied axial load conditions, which means the two sets of data are compared without considering the effects of the stress concentration that occurs at the trailing edge of contact. However this method for comparing data, which only considers the contribution of stress from the applied axial load, can be misleading. Therefore in the next Chapter, fatigue parameters are evaluated that incorporate the effects of the stress concentration.

First of all, the comparison of plain fatigue data for room and elevated temperature data, which is obtained from military handbook [30] for Ti-6Al-4V, is shown in Figure 3.13. The reason of presenting this data is to show that 260 °C temperature doesn't change the life of this material. The data shown in Figure 3.13 were obtained from 200-310 °C. These results validate the observation, which is presented at the following paragraphs in detail, that until 260 °C, the fatigue life data of Ti-6Al-4V at elevated temperature falls into a small scatter band of room temperature data. Furthermore the few plain fatigue experiments that are conducted in this study show the same kind of characteristic, as shown in Figure 3.14. The results of the elevated temperature plain fatigue experiments are shown in Table 3.2. This table of the experimental data provides: specimen number, the axial stress change, $\Delta\sigma_{axial}$, total number of cycles to rupture, N_f, the maximum axial stress, $\sigma_{axial,\max}$, the minimum axial stress, $\sigma_{axial,\min}$. It should be noted that the maximum number of cycles, that a test is subjected to, is 4×10^6 cycles. After this validation of the experiments by comparing the military handbook results and the results that are found in this study, the fretting fatigue study is presented in the following paragraphs and a comparison is made between the room temperature fretting fatigue data and the elevated temperature fretting fatigue data.

Figure 3.15 shows the elevated temperature fretting fatigue data expressed as the effective stress amplitude, $\sigma_{effective} = \sigma_{\max}(1-R)^m$, versus the number of cycles to specimen rupture. Here R is the ratio of minimum stress value to the maximum stress value, $R = \dfrac{\sigma_{\min}}{\sigma_{\max}}$ and it is 0.1 for this study, and it is kept constant throughout each test in this study. Another parameter, m is the fitting parameter and it is evaluated from plain

31

fatigue data, and was found to be equal to 0.45 in this study. Another comparison

method, which can be used, is the stress amplitude, $\Delta\sigma = \sigma_{max} - \sigma_{min}$. Figure 3.16 shows

the elevated temperature fretting fatigue data expressed as $\Delta\sigma = \sigma_{max} - \sigma_{min}$, versus the

number of cycles to specimen rupture.

Since the interest here is the fretting fatigue at elevated temperature, a comparison

is made between the room temperature fretting fatigue data and the elevated temperature

fretting fatigue data of the same pad radius. Figure 3.17 shows the fretting fatigue data

expressed as $\sigma_{effective}$ for both room and elevated temperature, and Figure 3.18 shows the

fretting fatigue data expressed as $\Delta\sigma$ for both room and elevated temperature. Note here

that at both figures the test frequencies are different. Also it is known from previous

study [18] that the frequency does not affect the fretting fatigue life of this material. To

conclude, the data for the elevated temperature fretting fatigue experiments falls into a

small scatter band of the data of room temperature fretting fatigue experiments. Note here

that a good comparison can be seen in Figure 3.17, and this figure shows the fretting

fatigue data expressed as $\sigma_{effective}$. This same result can be seen in Figure 3.13 and Figure

3.14 that show the plain fatigue data for elevated temperature data. It can be concluded

that 260 $°C$ temperature doesn't effect fretting fatigue behavior of this material

dramatically.

Before closing this discussion here, the comparison of the data of plain and

fretting fatigue for both room and elevated temperature must be presented together.

Figure 3.19 shows the fretting fatigue and plain fatigue at room temperature data

expressed as the effective stress amplitude, $\sigma_{effective} = \sigma_{max}(1-R)^m$, versus the number of

cycles to specimen rupture. Also another comparison based on, $\Delta\sigma = \sigma_{max} - \sigma_{min}$ is

shown in Figure 3.20. Furthermore, Figure 3.21 shows the fretting fatigue and plain

fatigue at elevated temperature data expressed as the effective stress amplitude versus the

number of cycles to specimen failure, and Figure 3.22 shows these same data expressed

as $\Delta\sigma$ versus the number of cycles to specimen failure. These figures indicate that the

relationship between fretting and plain fatigue at elevated temperature has the same

characteristics as the room temperature fretting and plain fatigue relationship.

In summary, it is seen that 260 $°C$ temperature does not have detrimental effect

on the fretting fatigue behavior of Ti-6Al-4V, but it is known from the literature [30] that

after 260 $°C$, the higher temperatures effect the properties of Ti-6Al-4V dramatically.

Further, as mentioned at Chapter II, Schaefer [24] found that elevated temperature (350

$°C$) had little detrimental effect on Ti-6Al-4V. These same results can be seen in the

parameter studies too. These results are shown in the next Chapter.
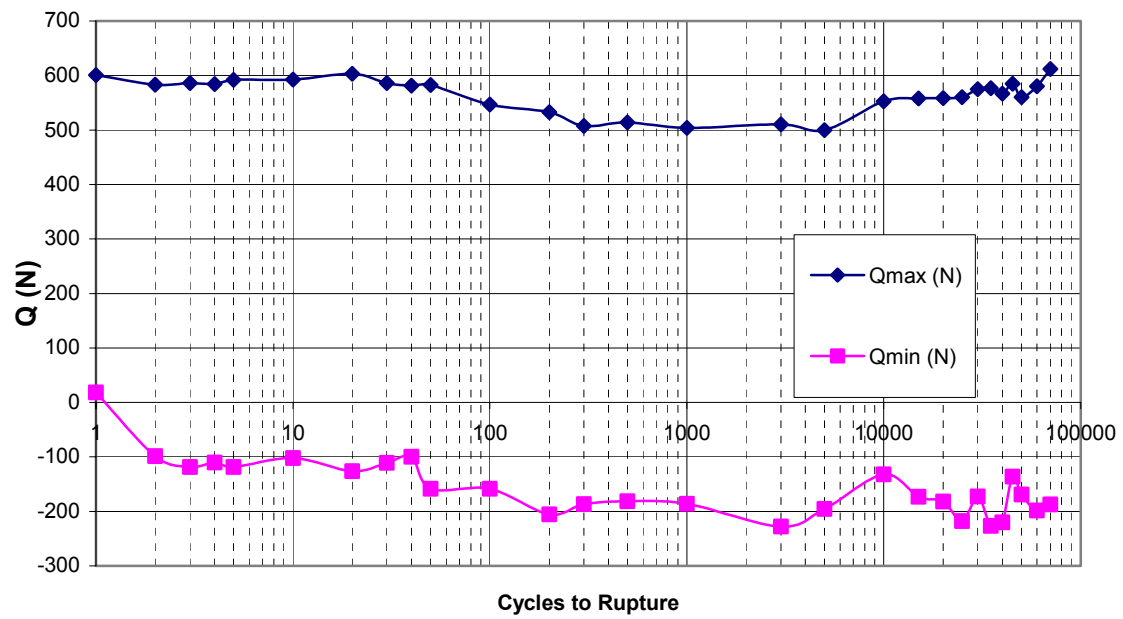
Figure 3.1. Typical Cycles versus Q Illustration.
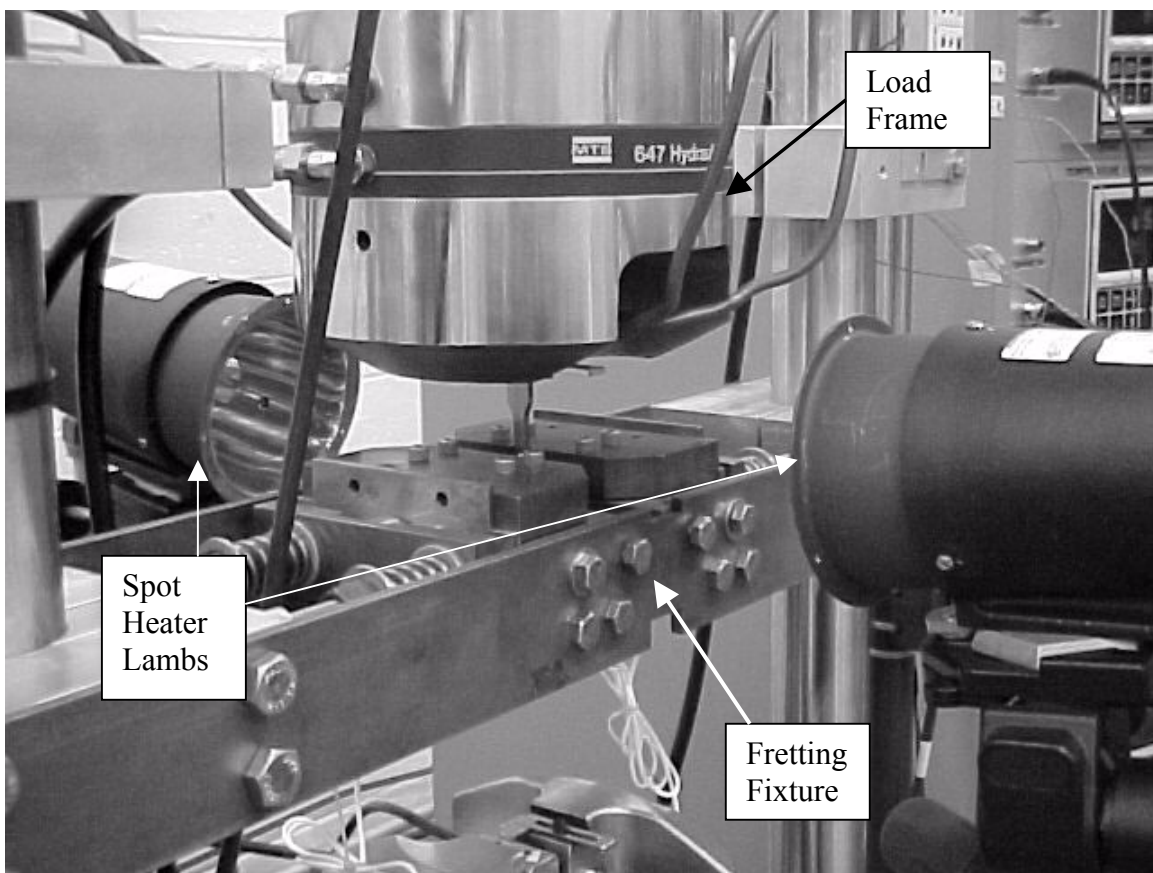
Figure 3.2. 22.2 kN Servohydraulic Load Frame and the Fretting Fixture.
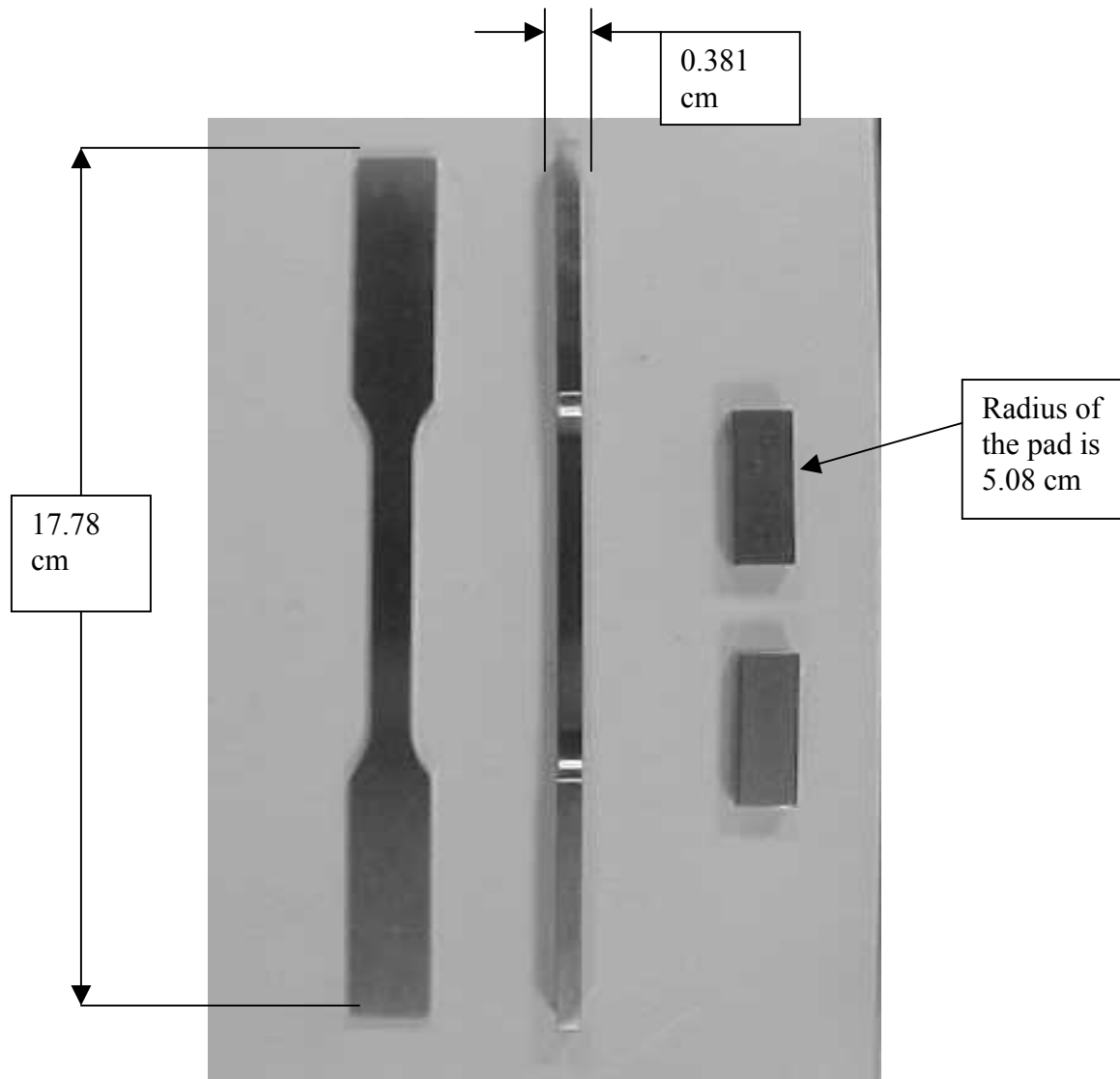
Figure 3.3. Specimen and Pads Used in This Research.
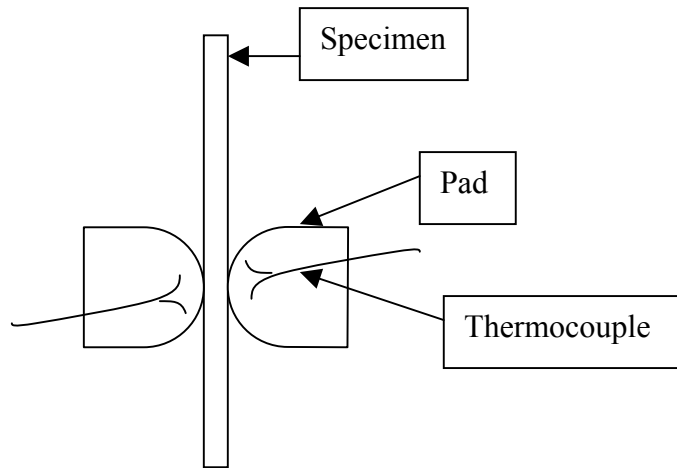
Figure 3.4. Illustration of Temperature Control by Thermocouples.
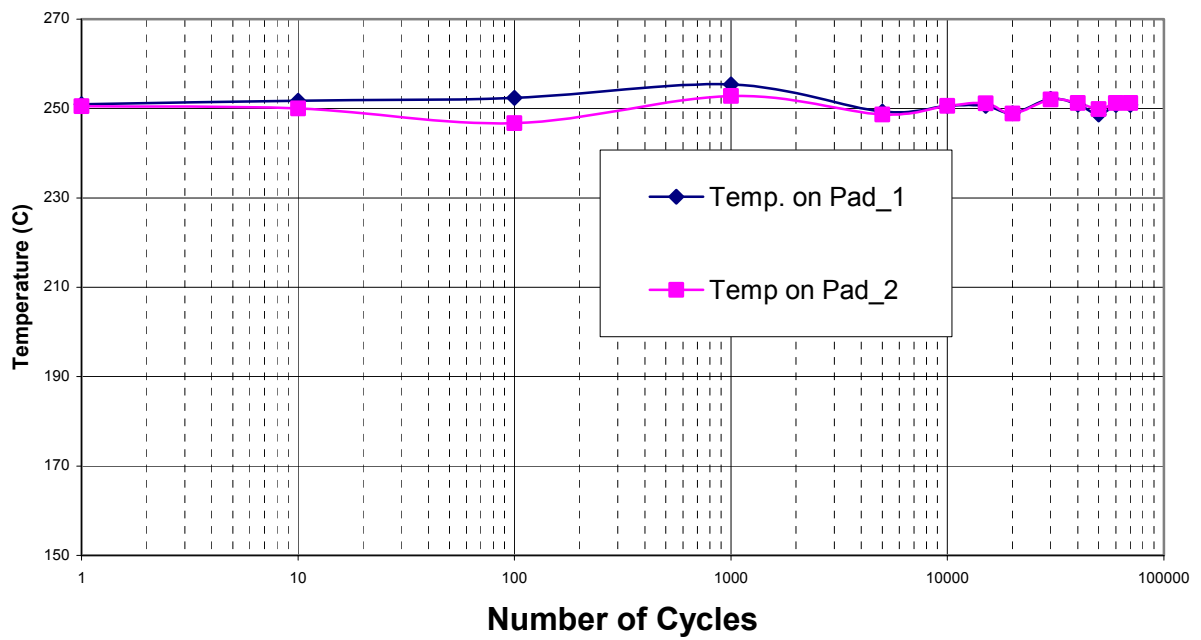
Figure 3.5. A Typical Temperature Profile on Pad Configuration.
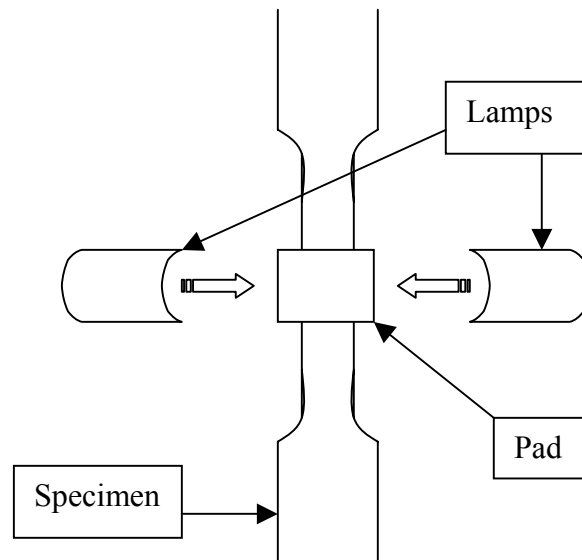
Figure 3.6. Configuration of the Lamps.
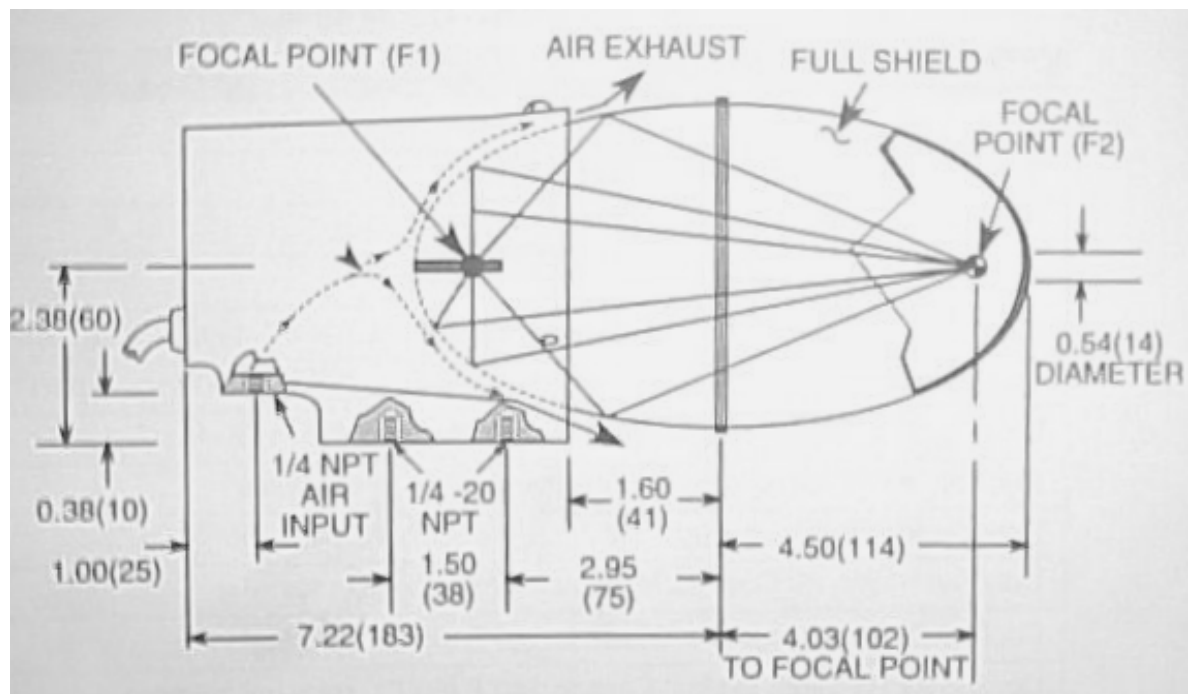
Figure 3.7. Configuration of the Spot Heater. (Dimensions are in Inch, and Numbers in Parenthesis are mm)
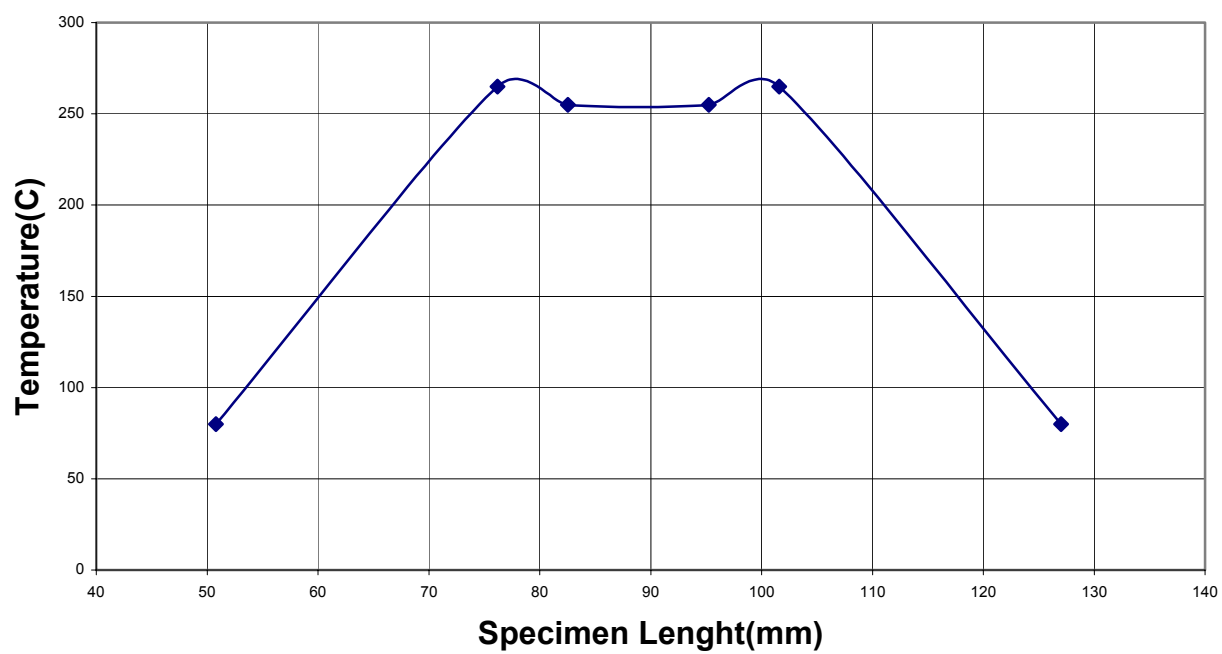
Figure 3.8. Temperature Analysis on Specimen.
(Note here total specimen length is 177.8 mm)
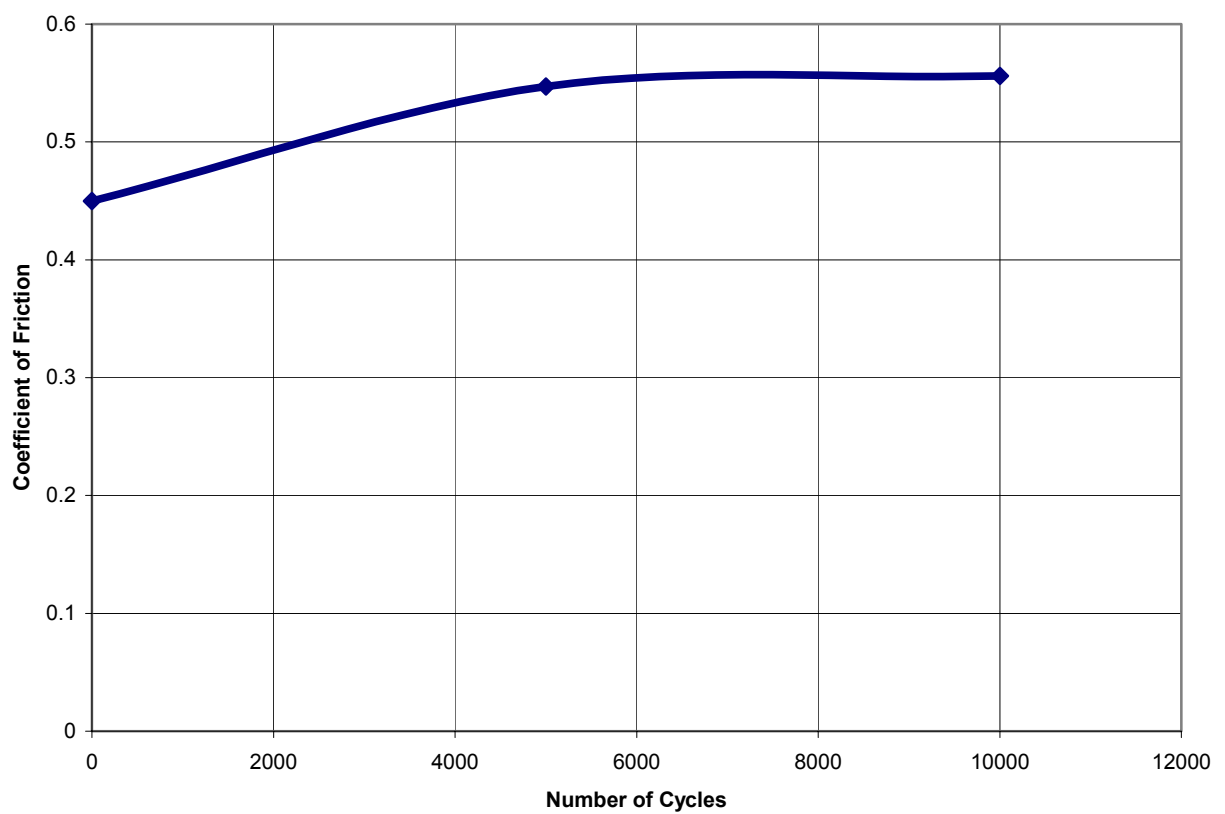
Figure 3.9. Coefficient of Friction Determination at Different Cycles at Elevated
Temperature.
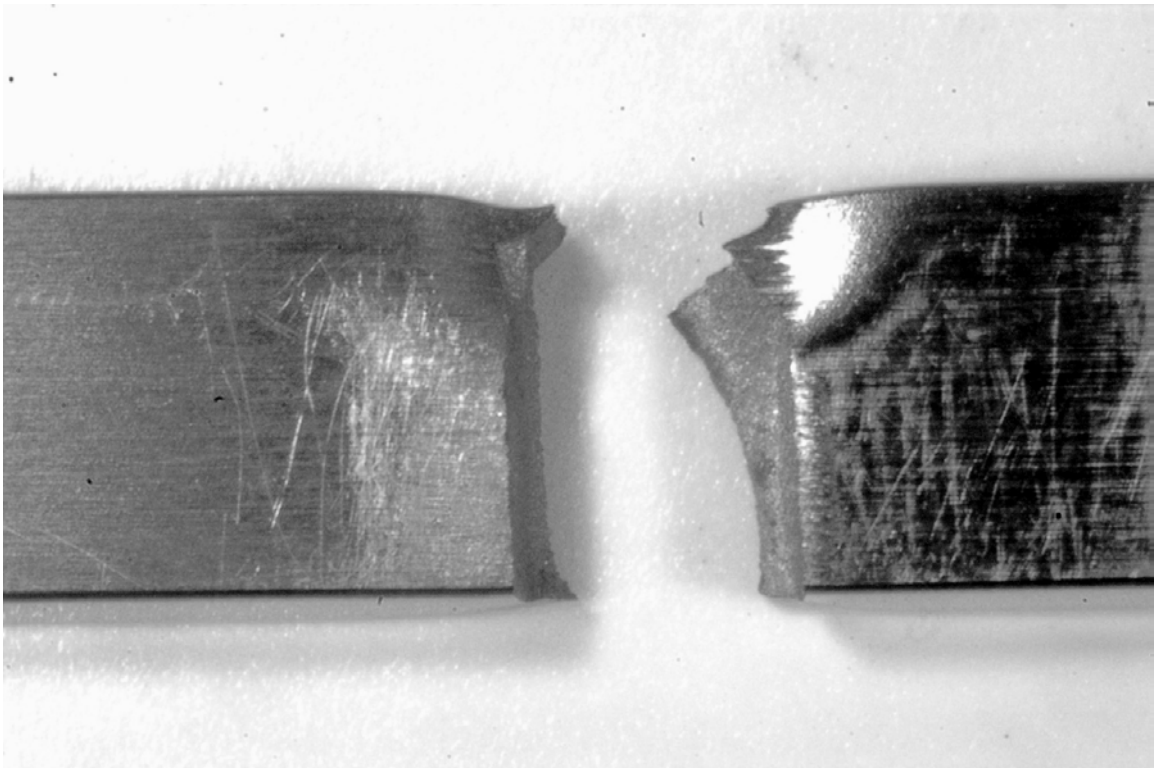
Figure 3.10. Failed Specimen.
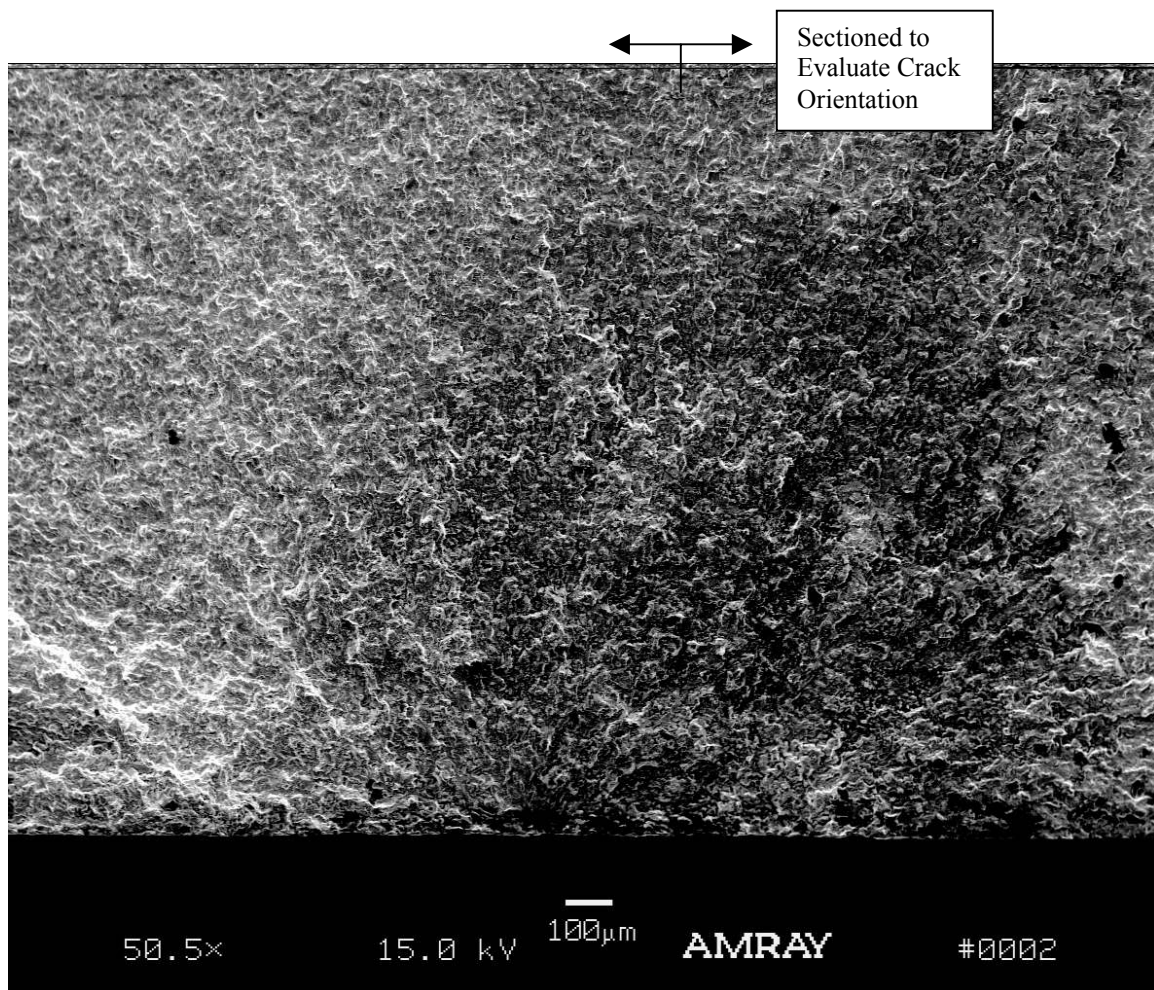
Figure 3.11. Crack Initiation Zone and Sectioning Direction.
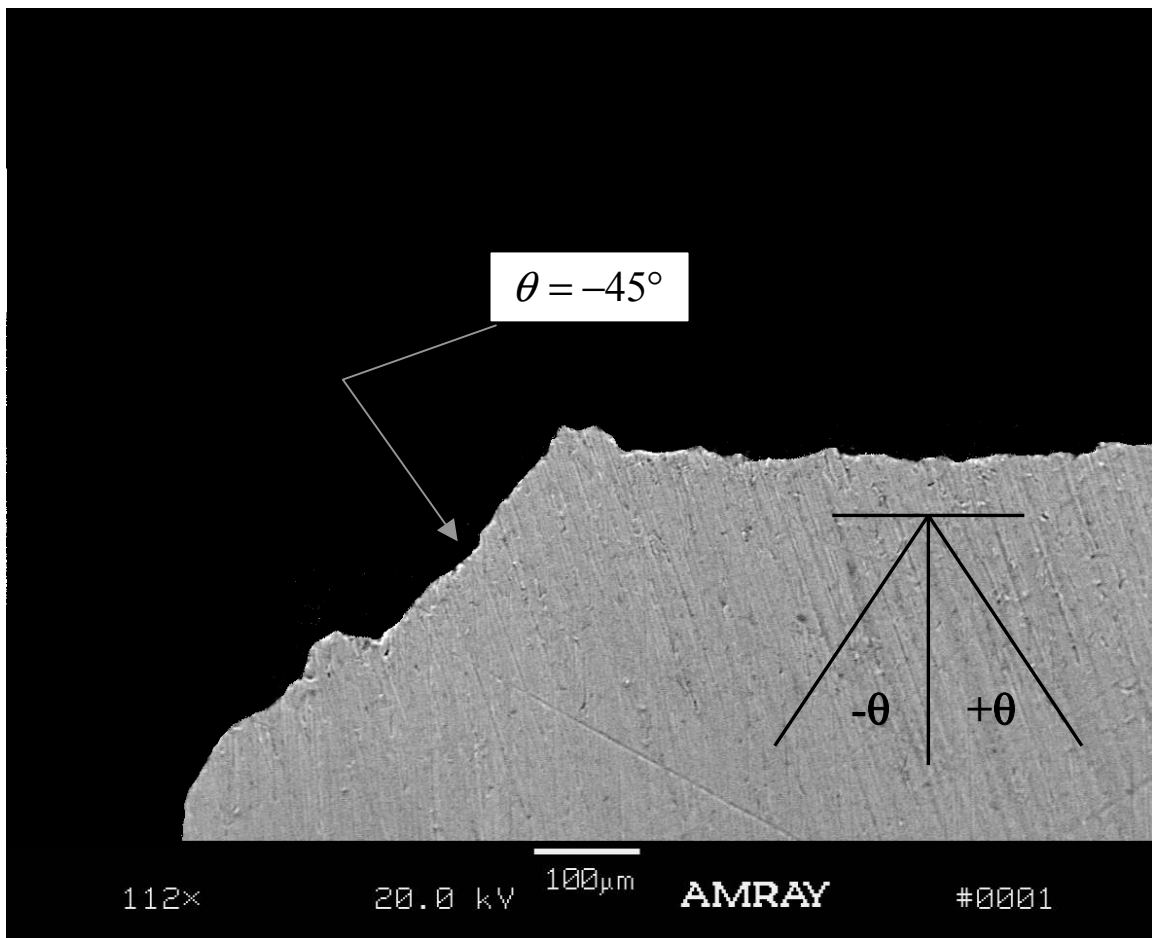
Figure 3.12. Crack Orientation.
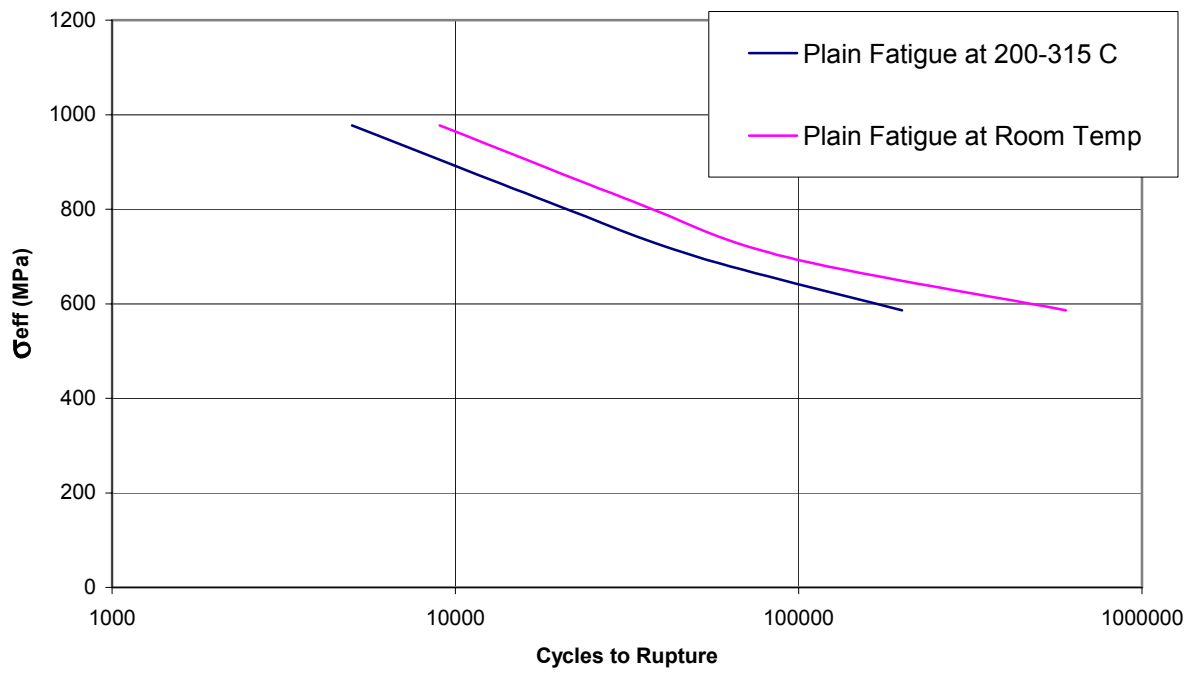
Figure 3.13. Comparison of Room and Elevated Temperature for Plain Fatigue
(From Handbook [30]).
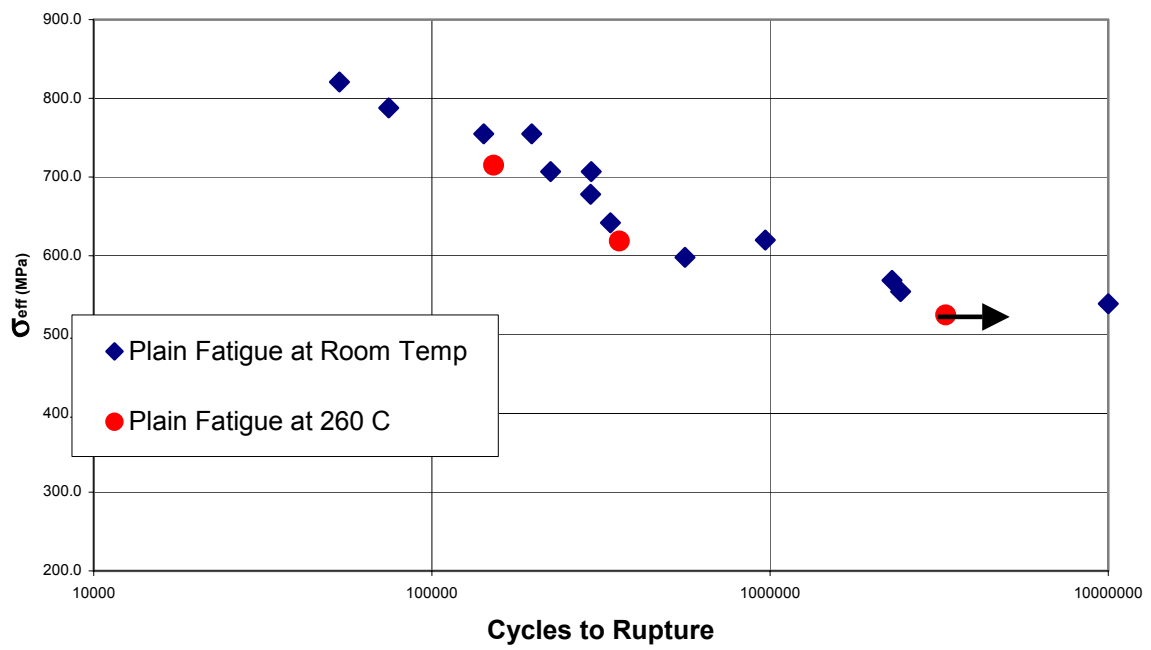
Figure 3.14. Comparison of Room and Elevated Temperature for Plain Fatigue
(This Study).
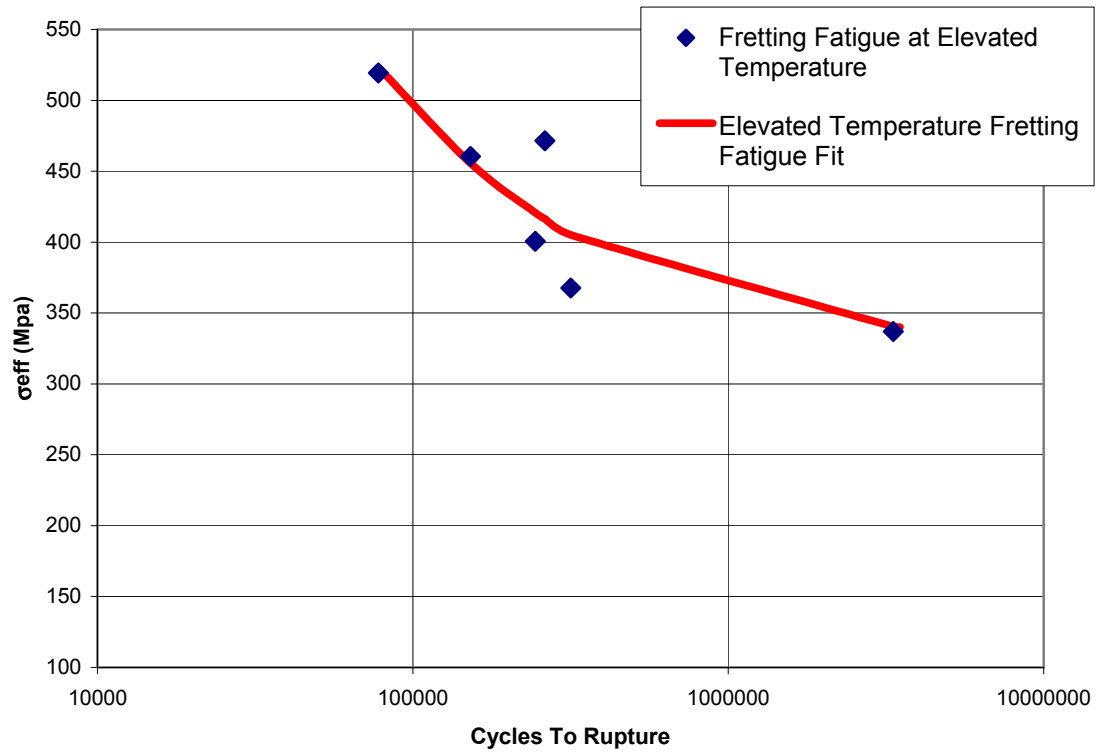
Figure 3.15. Fretting Fatigue Data for Elevated Temperature, $\sigma_{effective}$ versus N_f.
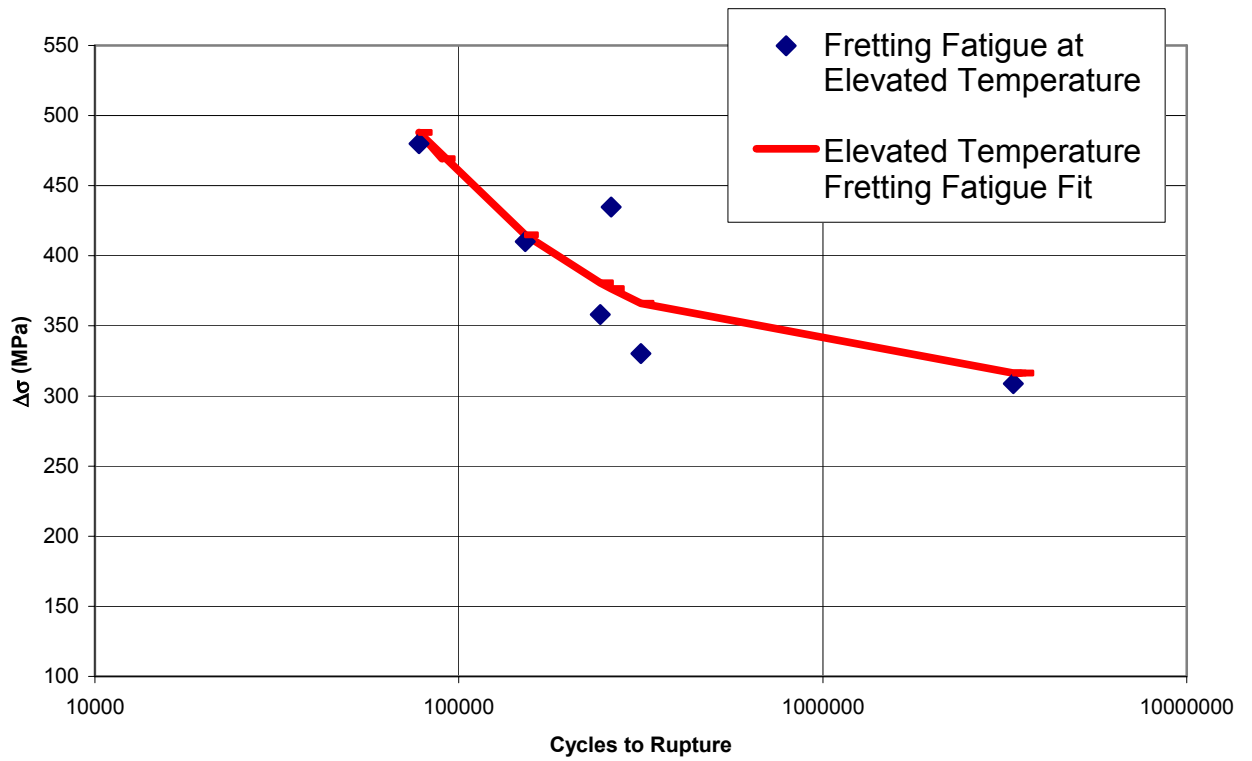
Figure 3.16. Fretting Fatigue Data for Elevated Temperature, $\Delta\sigma$ versus N_f .
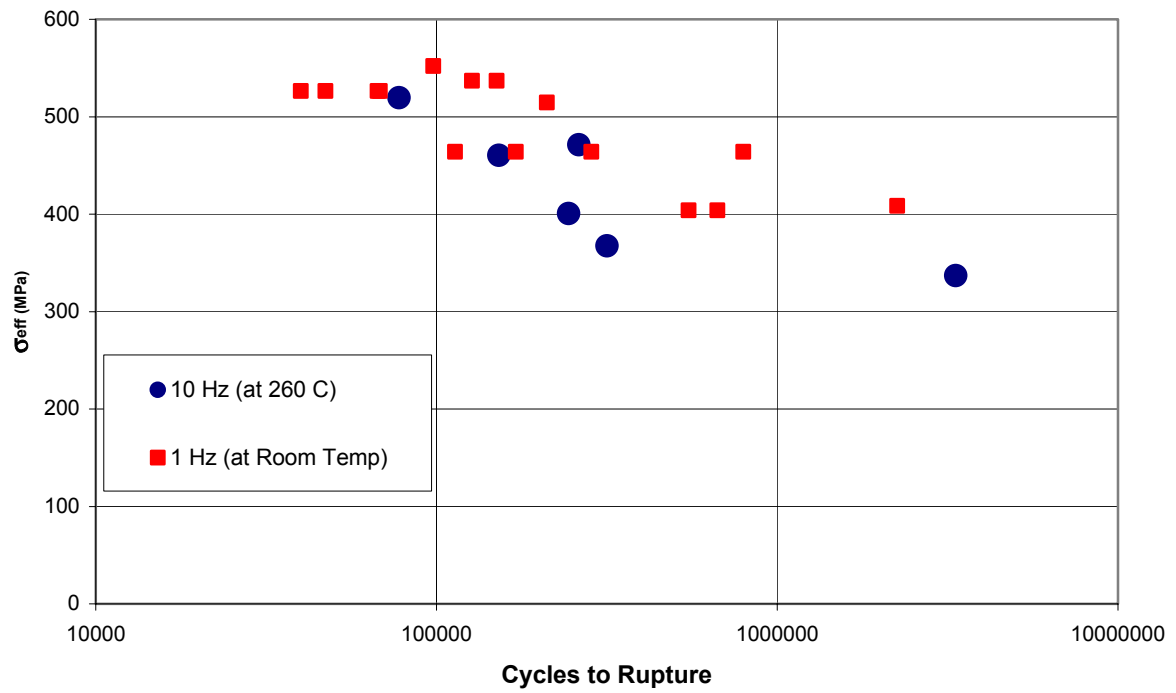
Figure 3.17. Comparison of Room and Elevated Temperature Fretting Fatigue Data, $\sigma_{effective}$ versus N_f.
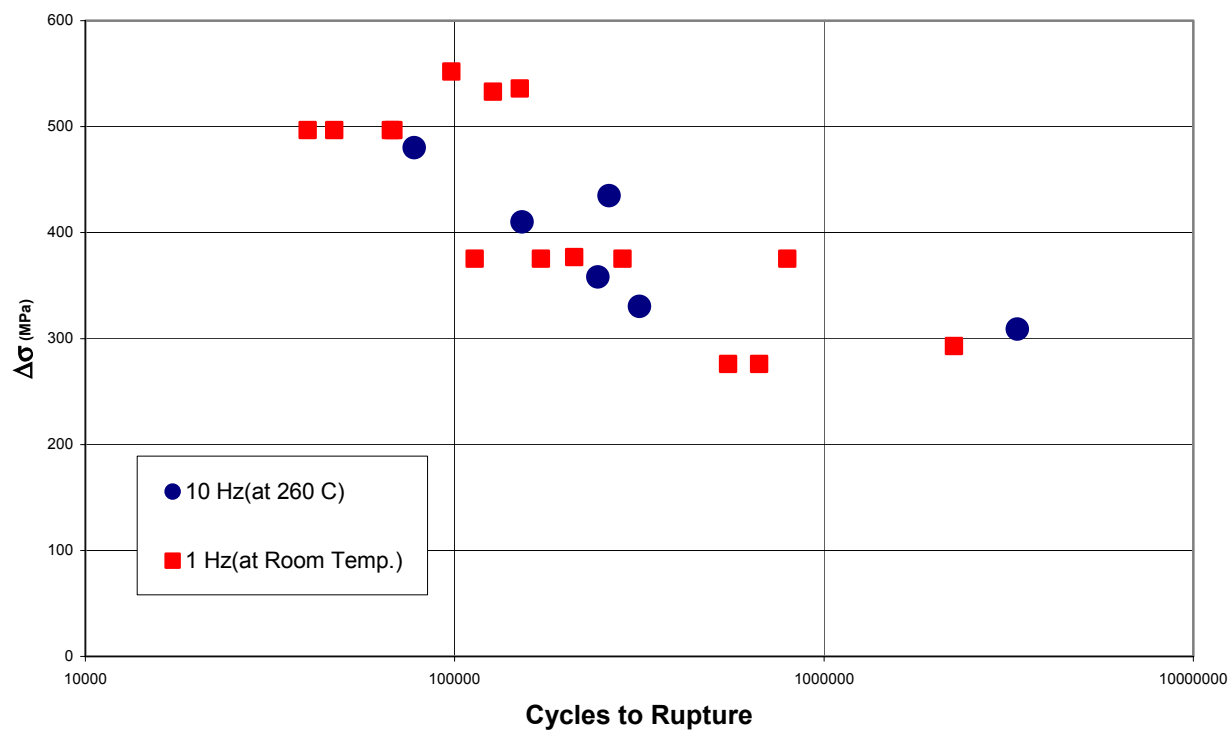
Figure 3.18. Comparison of Room and Elevated Temperature Fretting Fatigue Data,
$\Delta\sigma$ versus N_f.
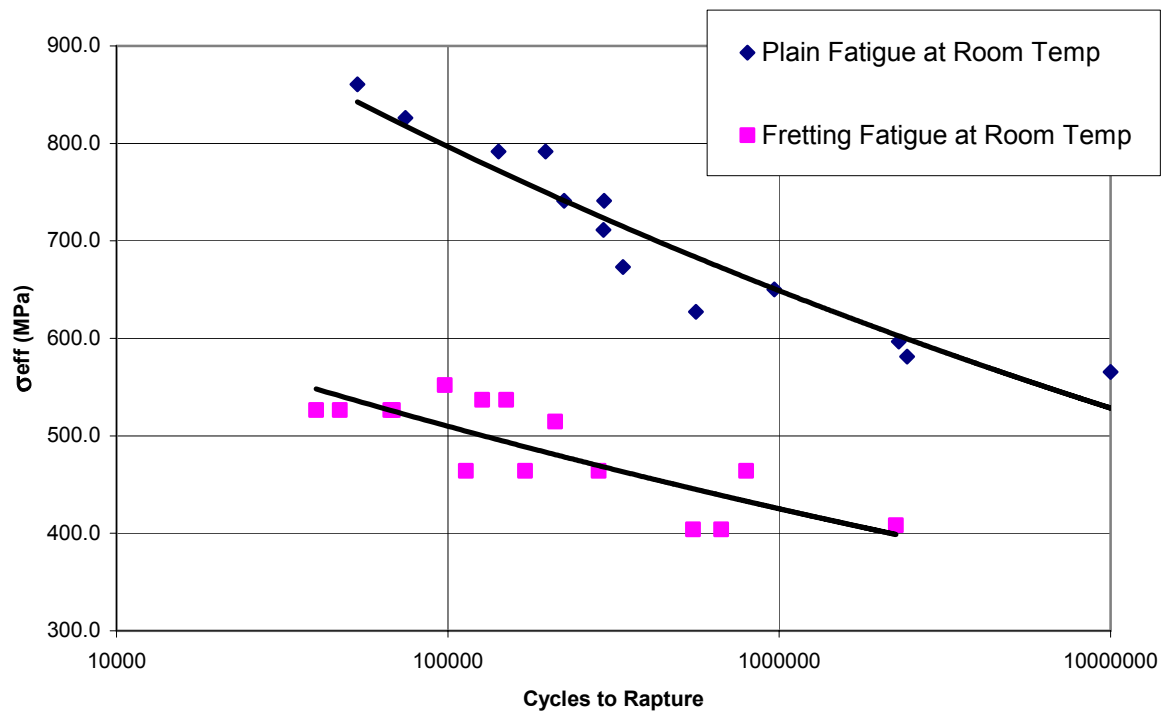
Figure 3.19. Comparison of Plain and Fretting Fatigue for Room Temperature, σ_{eff} .
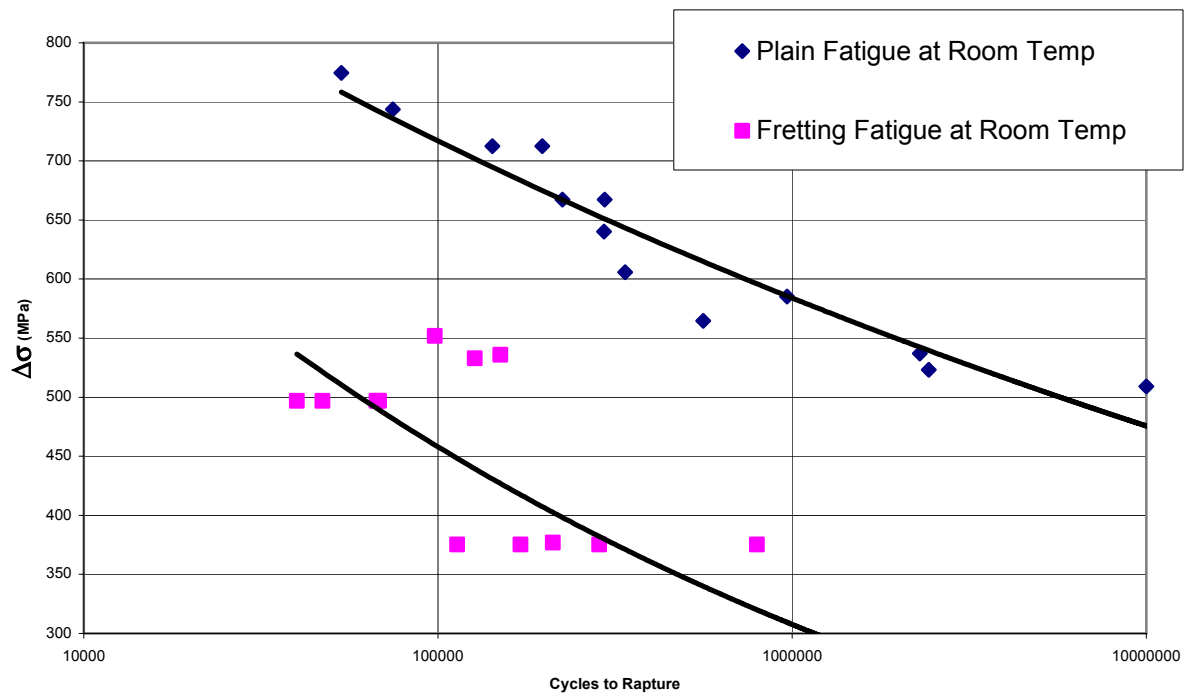
Figure 3.20. Comparison of Plain and Fretting Fatigue for Room Temperature, $\Delta\sigma$.
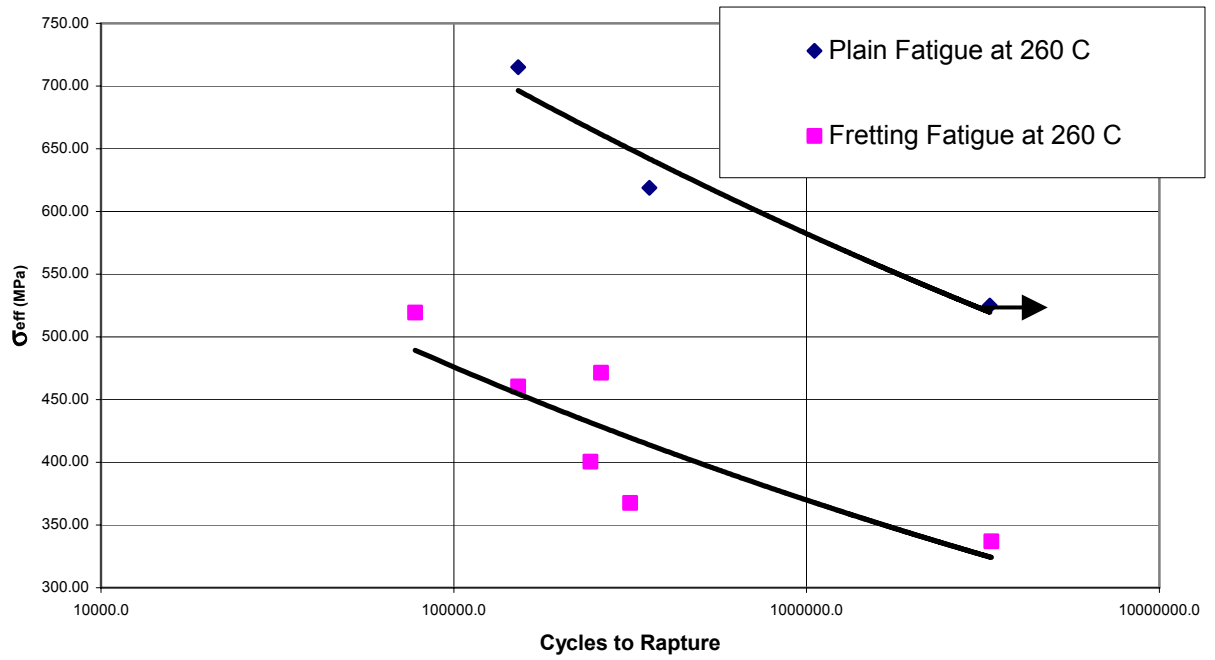
Figure 3.21. Comparison of Plain and Fretting Fatigue for Elevated Temperature, σ_{eff} .
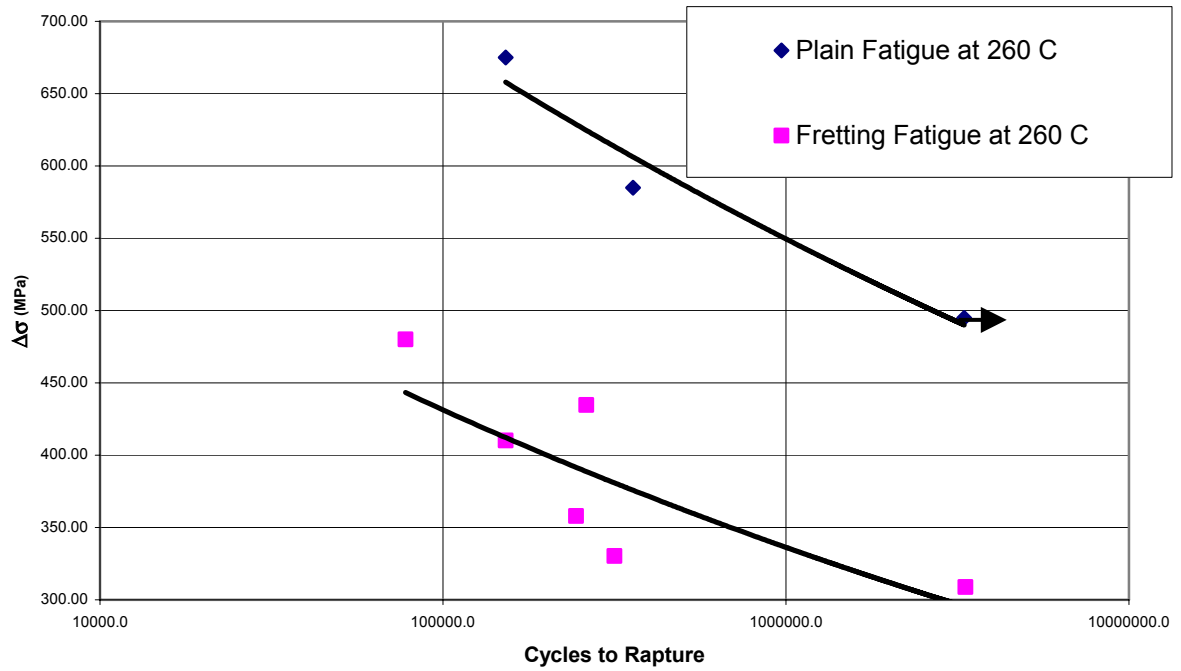
Figure 3.22. Comparison of Plain and Fretting Fatigue for Elevated Temperature, $\Delta\sigma$.

Table 3.1. Fretting Fatigue Test Data Summary at Elevated Temperature.

	N_f (cycles)	$\sigma_{axial,max}$ (MPa)	$\sigma_{axial,min}$ (MPa)	$\Delta\sigma_{axial}$ (MPa)	Q_{max} (N)	Q_{min} (N)
Specimen 1 (Failed at Thermocouple)	25641	550	50	500		
Specimen 2 (Failed at Thermocouple)	28672	550	50	500		
Specimen 3	77732	554	73.91	480	585	-220
Specimen 4	Stopped at 1795914	444.21	59.021	385.18	461	-127
Specimen 5	261755	503.6	68.766	434.83	470	-165
Specimen 6	244338	439.25	81.269	357.98	470	-89
Specimen 7	152341	506.18	95.97	410.21	483	-177
Specimen 8	316513	401.2	70.97	330.3	720	60
Specimen 9	Stopped 1825151	321	45.96	275	645	-88
Specimen 10	3338962	362.21	53.321	308.8	505	-90

Table 3.2. Plain Fatigue Test Data Summary at Elevated Temperature.

	N_f Cycles	$\sigma_{axial,max}$ (MPa)	$\sigma_{axial,min}$ (MPa)	$\Delta\sigma_{axial}$ (MPa)
Specimen 1	152323.0	750.00	75.00	675.00
Specimen 3	358243.0	650.00	65.00	585.00
Specimen 2	3307000.0	550.00	55.00	495.00

IV. Fatigue Parameter Analysis

In this chapter, fretting fatigue parameters capable of predicting the number of cycles to specimen failure, the crack location and the crack orientation along the contact surface are analyzed. There have been many fatigue life parameters in fretting fatigue as well as in multi-axial fatigue loading conditions proposed by various researchers. This study looks at four of these parameters, which depend on different local stresses or combinations thereof. First of all, the Smith-Watson-Topper parameter, which is based on the normal stress at a critical plane, is discussed. Second, shear stress range critical plane parameter, which is based on the shear stress range at a critical plane, is discussed. Lastly two parameters of discussion are the Findley Parameter and Modified Shear Stress Range (MSSR) parameters that are based on the combination of local shear and normal stresses. Each of these parameters is developed with particular emphasis on the region of the stress concentration that occurs along the surface at the trailing edge of contact.

In order to evaluate these parameters, finite element analysis (FEA) is conducted to model the experimental conditions (Table 3.1). For this reason before going through the discussion of parameters, FEA and validation of the finite element models is discussed. The finite element method is used to determine stress, strain and displacement fields at the contact interface. The salient features of the analysis are: four node, plane strain quadrilateral elements, which are used with the "master-slave" interfacial algorithm developed for contact modeling in the finite element code, ABAQUS [31]. The loads that are determined at Chapter III (Table 3.1) are applied to the model in two steps, and for each test the model is run twice, one for the maximum load application and other for the

56

minimum load application. The normal load, P is applied in the first step. In the second

step, the maximum tangential load Q_{max} and the maximum axial stress $\sigma_{axial,max}$ are

applied in the first run, and the minimum tangential load Q_{min} and the minimum axial

stress $\sigma_{axial,min}$ are applied in the second run. After this short discussion on the finite

element model that is used in this study, next two sections, which are about validation of

the finite element model and contact modeling with ABAQUS, are discussed in detail.

Contact Modeling With ABAQUS

The finite element method is a numerical procedure for analyzing structures and

continua [32]. It is a method in which a continuum body is *discretized* into a finite

number of elements. What happens basically is that these elements consist of nodes and

the equations that govern the problem can be defined as $n \times n$ equations and unknowns,

and by solving these equations the displacements and loads of the nodes can be solved.

The problem of elasticity can be formulated by considering the potential energy of a

continuous elastic system. This system of equations can be written in the following form

$$\Pi(u^N) = \int_V 1/2\{\varepsilon\}^T \{\sigma\}dV - \int_V \{u\}\{f\}dV - \int_{\partial V_\sigma} \{u\}^T \{t\}dA \qquad (17)$$

Where $\Pi(u^N)$ represents the kinematically admissible displacement states, the

first integral is the strain energy, the second term represents the internal forces and the

third integral represents the external tractions. This potential energy can be minimized in

order to solve for the displacements.

In this study, ABAQUS [31] program is used to model the contact analysis of this

research. The finite element analysis used in this research is very similar to the one

employed by Lykins [19] and also by Shantanu et al [34]. As mentioned before, four

node, plain strain quadrilateral elements are used with the "master-slave" interfacial

algorithm developed for contact modeling in ABAQUS. A similar study was employed

by Mcveigh and Farris [35]. However in their study eight node, plane strain quadrilateral

elements with gap elements at the interface were used. In this study four node elements

are chosen over eight node elements, because the mid-side node in the eight node element

introduces an oscillation in the stress state along the contact interface. The software

creates contact points by creating anchor points on the master surface. It locates the

anchor points by drawing a unit normal from the slave surface nodes to the master

surface. The slave nodes are then required to deform in relationship to the anchor points.

The Lagrange multiplier potential can be written as

$$\Pi_L(p, u^N) = pA'h'(u^N) \tag{18}$$

where p is the contact pressure, A' is the contact area and h' is the contact constraint,

which describes the amount of penetration that occurs between the two bodies in contact.

If it is determined that an anchor point and slave node pair are in contact, then the contact

constraint is enforced and Lagrange multiplier potential is used to determine the contact

parameters, such as pressure and slip, for this node pair.

Validation of Finite Element Model Configuration

Figure 4.1 shows the finite element model configuration. The finite element

model consists of three bodies. The first body is a rigid body constraint, the second body

is the fretting pad and the third body is the fretting specimen. In order to compare the

finite element analyses to other analytical solutions the thickness of the fretting fatigue

58

specimen is increased about six times of its original thickness to make it as the half space, to simulate the analytical condition required for this comparison.

The load conditions that are applied to the system are shown in Figure 1.3. The boundary conditions for this configuration is that fretting pad is constrained in the x and y direction by the rigid body constraint. There is also a multi-point constraint applied to the top of the pad to keep it from rotating due to the application of loads. Nodes along this constraint line are forced to move in unison in the y-direction. Fretting specimen and the half space are constrained in the x and y direction. The axial stress is applied to the right hand side of the specimen and half space, the normal load is applied at the top of the pad and the tangential load is applied on the left hand side of the fretting pad. A small sliding contact condition is used between the fretting specimen and fretting pad. This kind of contact condition is necessary for the type of analysis required for fretting fatigue, because this condition establishes the contact algorithm for the transfer of loads between the bodies in contact.

As mentioned before, the loads are applied to the model in two steps, and for each test the model is run twice, once for maximum load application and for minimum load application. Lykins [19] found that the multiple cycling didn't change the results found after one cycle. For this reason, all computations for this study are conducted over one fatigue cycle.

In addition to these considerations, temperature analysis in the ABAQUS model is conducted. This is done to investigate the changes in the model output with temperature as used in this study. Temperature analysis can be conducted in different ways with ABAQUS program. Since these different ways are discussed in Appendix B, only the

method that is used in this study is mentioned here. In FEA model that is used in this study, the room temperature is applied or defined in the program before applying loads. Then, the temperature that is the concern here is applied in two different ways in order to compare their differences. First, $260\,°C$ is applied before the normal load is applied to the system. Also, as a second case $260\,°C$ is applied after the normal load is applied to the system. The concern here is to investigate the difference in the stress concentration at the contact area as a result of the temperature. This analysis shows that the results are same with the ones that are conducted without temperature for the same load condition. This result is due to the free end of the specimen (on one side). For this reason, in this study all computations are conducted without applying any temperature to the system. However, the change in the Young's modulus of the material due to temperature is considered in the model.

Finally, Figure 4.2 shows the variation of the normal stress in the x-direction along the contact surface for the Chan and Lee solution [29], the half space solution, and the actual specimen thickness used for this research. There is good agreement between the Chan and Lee solution and the results of the FEA half space solution as can be seen in Figure 4.2. The predicted maximum normal stress in the x-direction varied by 5%, $\sigma_{xx,FEA} = 776$ MPa versus $\sigma_{xx} = 737$ MPa. Furthermore, the predicted contact half width varied only by 0.16%, $a_{FEA} = 471.2$ μm versus $a = 472$ μm. After this validation of the FEA model, investigation into fatigue parameters is discussed next.

Smith-Watson-Topper (SWT) Critical Plane Approach

Previous researchers have used the SWT parameter to predict the fatigue life in steels and aluminum alloys under the multi-axial fatigue loading condition [36]. Szolwinski and Farris [37] modified the SWT parameter for application to fretting fatigue crack initiation. The modified Smith-Watson-Topper parameter for the fretting fatigue crack initiation assumes that crack initiation occurs on the plane where the product of normal strain amplitude, ε_a and maximum normal stress, σ_{max} is the maximum. To calculate this parameter the computed stresses and strains from the finite element of the fretting fatigue experiments are used. In this parameter, the critical plane is defined as the plane where the modified SWT parameter is a maximum. Thus, the critical plane approach using this parameter provides the location and the orientation of the crack initiation in fretting fatigue. In this work, the modified Smith-Watson-Topper critical plane parameter is calculated in steps of 0.1^o at angles ranging from $-90°$ to $90°$ from the perpendicular to the applied bulk stress. The definition of this angle is shown in Figure 3.10. This calculation provides SWT parameter's maximum value location and critical plane orientation. Table 4.1 shows the results of this parameter analysis for elevated temperature fretting fatigue conditions.

Figure 4.3 shows the measured fretting fatigue life data at elevated temperature as a function of Smith-Watson-Topper parameter along with the plain fatigue and fretting fatigue at room temperature data. Figure 4.3 clearly shows that fretting fatigue crack initiation at elevated temperature life data lie within a small scatter band of the plain fatigue and fretting fatigue at room temperature life data. Furthermore, SWT Parameter is calculated for elevated temperature plain fatigue conditions, and results of this calculation

are shown in Table 4.4. Also, plain fatigue life data for elevated temperature are plotted

as a function of this parameter in Figures 4.3 and 4.4, along with the corresponding

relationship for the room temperature plain fatigue data. These figures again show a good

agreement between the experimental result that is found at Chapter III and this parameter

analysis also shows that the 260 $°C$ temperature does not have detrimental effect on

Ti-6Al-4V.

Both figures indicate that fretting and plain fatigue at elevated temperature data

lie within a small scatter band of plain and fretting fatigue at room temperature data. In

other words, the fretting fatigue crack initiation life for elevated temperature can be

predicted from the Smith-Watson-Topper parameter versus fatigue life relationship of the

plain fatigue.

The crack location and the angle of initiation are also two important

considerations in the evaluation of any parameter. The predicted crack location is

determined to be near the trailing edge of the contact based on this approach, which is in

good agreement with experimental observations. However, the SWT parameter predicts

the angle of crack orientation at the contact surface as within –0.4° to +0.1° of the

perpendicular to the applied loading direction. This is not in agreement with the

experimental observation of the crack initiation angle of - 45°.

In conclusion, Smith-Watson-Topper parameter has the limitation of not

predicting the crack orientation. However, the parameter is in good agreement with

experimental observations with respect to crack location, and Smith-Watson-Topper

parameter versus fatigue life relationship of the plain fatigue can be used to predict the

fretting fatigue crack initiation life for elevated temperature.

Shear Stress Range Critical Plane Approach

The next parameter that is considered in this study is based on the shear stress (τ) on the critical plane. The shear stress range, $\Delta\tau = \tau_{max} - \tau_{min}$, is computed on all planes at all points in the contact region which provides a critical plane where this range is a maximum. Here, τ_{max} and τ_{min} are the shear stress values due to the maximum and minimum applied axial loading respectively. In this approach, the maximum and minimum shear stresses on all planes ranging from $-90°$ to $90°$ in increments of 0.1 degree are considered. These maximum and minimum shear stresses are calculated by using the stresses and strains that are obtained from the finite element analysis. From this, the critical plane and magnitude of the maximum shear stress range $\Delta\tau_{crit} = \tau_{max} - \tau_{min}$ is obtained. In order to account for the effect of the mean shear stress ratio, a technique, which is proposed by Walker [38], is incorporated. This is expressed as:

$$\Delta\tau_{crit,effective} = \tau_{max}(1 - R_\tau)^m \tag{19}$$

where τ_{max} is the maximum shear stress on the critical plane, R_τ is the shear stress ratio on the critical plane, and m is a fitting parameter, which is determined to be 0.45 from the plain fatigue data.

Figure 4.5 shows the measured elevated temperature fretting fatigue life data as a function of the parameter $\Delta\tau_{crit,effective}$. Figure 4.6 shows same data as a function of Shear Stress Range, $\Delta\tau$ parameter. These figures clearly show that elevated temperature fretting fatigue data lie just below the room temperature fretting fatigue life data and lie on the plain fatigue data. In addition, the parameter $\Delta\tau_{crit,effective}$ for elevated temperature plain fatigue conditions is calculated, and results are shown in Table 4.4. Also, plain fatigue

63

life data is plotted for elevated temperature as a function of this parameter in Figures 4.5 and 4.7, along with the corresponding relationship for the room temperature plain fatigue data. Also Figures 4.6 and 4.8 show the $\Delta\tau$ parameter for the elevated temperature plain fatigue data. Note in these figures, elevated temperature plain fatigue data curve is in a very small scatter band of the room temperature data. This result is in good agreement with the experimental result. In addition to these four figures, Figures 4.9 and 4.10 show the scatter band of fretting fatigue data at room temperature with fretting fatigue data at elevated temperature. These two figures clearly show that fretting fatigue at elevated temperature data falls into $\pm 3N$ scatter band of plain fatigue at room temperature data, which means this parameter can be used to predict the elevated temperature fretting fatigue life from the plain fatigue data in conjunction with an analysis.

Table 4.2 shows the results of this parameter analysis for elevated temperature fretting fatigue conditions. As can be seen, the maximum shear stress range occurs on one plane in the positive quadrant, which is ranging from $41.5°$ to $44.5°$ from the perpendicular to the loading direction. It should be noted that the maximum shear stress range occurs on two planes, one in the positive quadrant (i.e. from 0^0 to 90^0 from the perpendicular to the loading direction, Figure 3.10) and the other in the negative quadrant (i.e. from 0^0 to -90^0 from the perpendicular to the loading direction). For each state of stress, there are thus two critical shear stress planes, which are at $90°$ to each other and either of the two orientations is equally possible, however local variation in microstructural properties may cause one orientation to be preferred. Also, the predicted crack initiation location agrees with the experimental results and it is determined to be near the trailing edge of the contact. To conclude, these results are in good agreement

with the experimental observations and this parameter can be used to predict the fretting fatigue crack initiation life, location and orientation at elevated temperature. In this study, the shear stress range critical plane parameter satisfactorily describes the fretting fatigue behavior of Ti-6Al-4V. However, a prior work [34] showed the dependence of this parameter on the fretting pad geometry. The results showed in that study point out limitations of this parameter with a large variation of geometry and peak normal stress.

As can be seen from the preceding discussion the fatigue life parameters based on the shear or normal stresses in the contact region does not satisfactorily describe the behavior of Ti-6Al-4V under fretting fatigue for various loading conditions and geometries. Generally for ductile metals, intense deformation due to shear motion between crystal planes creates slip bands, which lead to crack initiation. Therefore, on a micro-scale (of the order of the grain size), the local shear stresses may play a dominant role in the crack nucleation during fretting. However, for high cycle fatigue, crack initiation may be considered as the sum of two components: (1) crack nucleation, and (2) crack propagation from a nucleated size to a detectable size. Hence, it is reasonable to assume that the normal stress on the critical plane of crack nucleation may also play a role. A fretting parameter, which is a combination of shear and normal stresses on a critical plane, therefore, can describe the fretting fatigue of Ti-6Al-4V better than a fretting parameter that is based on only shear stresses or normal stresses. Therefore, parameters which are a combination of the local shear and normal stress are considered next.

65

Findley Parameter

Findley Parameter (FP), proposed by Findley [39] in the sixties, basically considers the effect of normal and shear stresses (strains). Because the crack initiation in the multi-axial fatigue loading should be influenced by both normal and shear stresses. In this approach, crack initiation is assumed to be governed by both the maximum shear stress amplitude, $\tau_a = (\tau_{max} - \tau_{min})/2$ and maximum stress normal to orientation of the maximum shear multiplied by an influence factor, k as shown in the following:

$$FP = \tau_a + k\sigma_{max} \tag{20}$$

Similar to what Lykins [19] and Shantanu et al [34] did, the Findley Parameter, FP is calculated at all planes ranging from $-90° \le \theta \le 90°$ in 0.1 degree from the computed stresses and strains obtained from the finite element analysis. These calculations provide the critical plane where this parameter is the maximum. Table 4.3 shows the results of this parameter analysis for elevated temperature fretting fatigue conditions.

The measured fretting fatigue crack initiation life data for elevated temperature are plotted as a function of this parameter (Figure 4.11), along with the corresponding relationship for the room temperature plain fatigue and fretting fatigue data. In addition, Findley Parameter for elevated temperature plain fatigue conditions is calculated, and results are shown in Table 4.4. Also, plain fatigue life data for elevated temperature are plotted as a function of this parameter in Figures 4.11 and 4.12, along with the corresponding relationship for the room temperature plain fatigue. Note here that the elevated temperature Findley Parameter data is in a very small scatter band of the room temperature data. This result is in good agreement with the experimental result. For this case, the FP versus life relationships for the fretting fatigue at elevated temperature falls

between the data for plain and fretting fatigue at room temperature. It can be therefore seen here that Findley parameter does not give a good relationship for fretting fatigue life relationships. Further, the relationship between fretting fatigue data for 50.8 mm pad at room temperature and at elevated temperature is not in agreement with the relationship that is observed in experiments. Also, crack initiation location that is predicted is near the trailing edge, which is in agreement with the experimental observation. However, the Findley parameter predicts the angle of crack orientation at the contact surface as within $-19.9°$ to $-25.5°$ of the perpendicular to the applied loading direction. This is not in agreement with the experimental observation of the crack initiation angle of $-45°$. This parameter studies show that elevated temperature fretting fatigue data fall into scatter band of room temperature data, but fretting fatigue at room temperature data do not fall into this scatter band. Also the crack orientations that are predicted by the help of FP are different from than those observed experimentally.

Therefore, to summarize, the Findley parameter predicts the crack location satisfactorily. However, it does not predict the crack orientation satisfactorily and in addition Findley parameter does not give a good fatigue life relationships. Even though, the elevated temperature fretting fatigue data fall into scatter band of room temperature plain fatigue data, room temperature fretting fatigue data do not fall into this scatter band, and a reliable fretting fatigue parameter must be capable of predicting these observations for all situations. For this reason this parameter cannot be used to predict the fretting fatigue crack initiation life, location and orientation at elevated temperature.

Modified Shear Stress Range (MSSR) Critical Plane Approach

To overcome this shortcoming of the Findley Parameter mentioned above, shear stress range critical plane parameter is modified in the form similar to Findley parameter to account the normal stress that generally aids in opening the crack surfaces. This modified version of shear stress range critical plane parameter can be expressed as follows:

$$\text{MSSR} = A.\Delta\tau^{B}{}_{crit} + C.\sigma^{D}{}_{max} \tag{21}$$

In this approach, the first term $\Delta\tau_{crit,effective}$ is the same as in equation (19) and the second term is the maximum normal stress on the critical plane. The constants A, B, C and D can be obtained by curve fitting.

Figure 4.13 shows the elevated temperature fretting fatigue life data as a function of the modified shear stress range parameter. As it can be seen in this figure that the elevated temperature fretting fatigue data lie very close to room temperature fretting fatigue data and lie within a small scatter band of the plain fatigue data.

In the region of longer fatigue life, the scatter between the data for different temperature fretting fatigue and plain fatigue is very small indicating that the plain fatigue data may be used to predict the fretting fatigue behavior using this parameter for the high cycle fatigue life region. Ideally, a parameter describing the fretting fatigue behavior should be able to correlate fretting fatigue with plain fatigue over the entire range of life. It should be noted in Figure 4.15 that the elevated temperature fretting fatigue data appears to deviate from the scatter band, especially in the low cycle fatigue life region. However, the author believes that a parameter based on a combination of

68

shear and normal stresses, like the MSSR, can be used to predict the fretting fatigue life from the plain fatigue data.

Furthermore, MSSR Parameter for elevated temperature plain fatigue conditions is calculated, and the plain fatigue life data for elevated temperature is plotted as a function of this parameter in Figures 4.13 and 4.14, along with the corresponding relationship for the room temperature plain fatigue data. These figures show the good agreement between the experimental observations and the FEA results, i.e. the 260 $°C$ temperature does not have detrimental effect on this material. Further, Figure 4.15 shows the $\pm 3N$ scatter band of room temperature plain fatigue data. This figure indicates that this parameter can be used to predict the elevated temperature fretting fatigue life from the room temperature plain fatigue data in conjunction with an analysis. In addition, angle of crack orientation and crack location that are predicted by this parameter are same as in the case of the shear stress range critical plane parameter, and these are in agreement with their experimental counterparts as it is stated above. For the sake of their relationship, the data of MSSR parameter is put with shear stress range parameter in Table 4.2 together.

Finally, this modified parameter explicitly includes the effects of the shear stress as well as normal stress as it is should be the case in the multi-axial fatigue loading, and also elevated temperature fretting fatigue data for MSSR parameter falls into scatter band of room temperature plain fatigue data. This clearly indicates that this parameter can be used to predict the fretting fatigue life from the plain fatigue data in conjunction with an analysis.

Summary of The Parameter Analysis

In this study several critical plane based multi-axial fatigue parameters are examined to investigate fretting fatigue crack initiation behavior in a titanium alloy, Ti-6Al-4V, at elevated temperature. All the parameters above are evaluated on their ability to predict the number of cycles to fretting fatigue crack initiation, crack initiation location and crack initiation angle along the contact surface. SWT parameter, which includes the effect of the normal stress, predicts the cycles to fretting fatigue crack initiation and crack location, which are in agreement with their experimental counterparts. However, its prediction of the crack orientation is not in agreement with the experimental observation. Another parameter, shear-cracking based critical plane parameter predicts the cycles to fretting fatigue crack initiation, crack initiation location and crack orientation which are in agreement with their experimental counterparts. Even though this parameter is in agreement with the experimental observations and predicts the elevated temperature fretting fatigue life well from the room temperature plain fatigue data, it is based on only shear stresses, and as mentioned before a fretting parameter, which is a combination of shear and normal stresses on a critical plane can describe the fretting fatigue of Ti-6Al-4V better than a fretting parameter that is based on only shear stresses or normal stresses.

Findley parameter, a critical plane approach involving both normal and shear stresses (or both tensile and shear cracking) predicts the fretting fatigue crack orientation which is not in agreement with the experimental observation. Further, Findley parameter does not give a good relationship for fatigue life relationships. However, a modified version of shear stress range parameter involving both normal and shear stresses (or both

70

tensile and shear cracking) predicts the cycles to fretting fatigue crack initiation, crack initiation location and crack orientation which are in agreement with their experimental counterparts.

From these observations, it is clear that the fretting fatigue crack mechanism in the tested titanium alloy at elevated temperature is governed by the shear stress on the critical plane. The normal stress on the critical plane seems to play a part in conjunction with the shear stress in the propagation of the crack. However, the exact role of the normal stress on the critical plane upon the fretting fatigue crack initiation behavior appears to be unclear from this study, and hence more experiments involving various temperature values, loading conditions, and different geometries are needed to investigate this phenomenon.
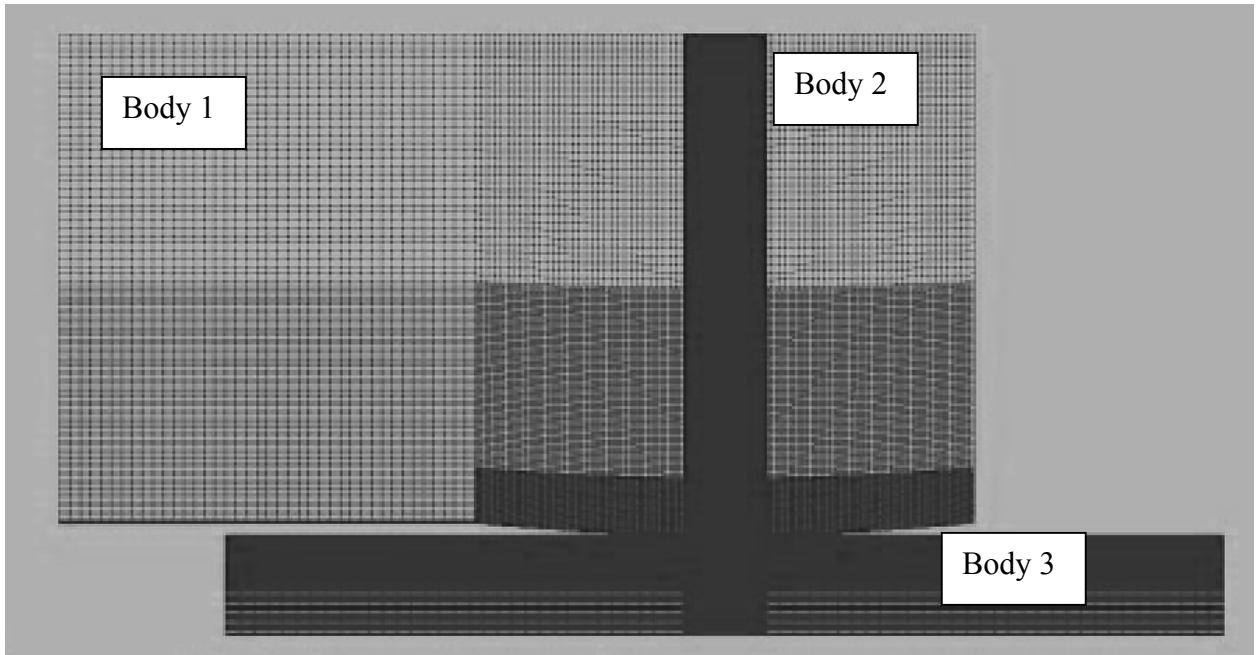
Figure 4.1. Finite Element Model Configuration.
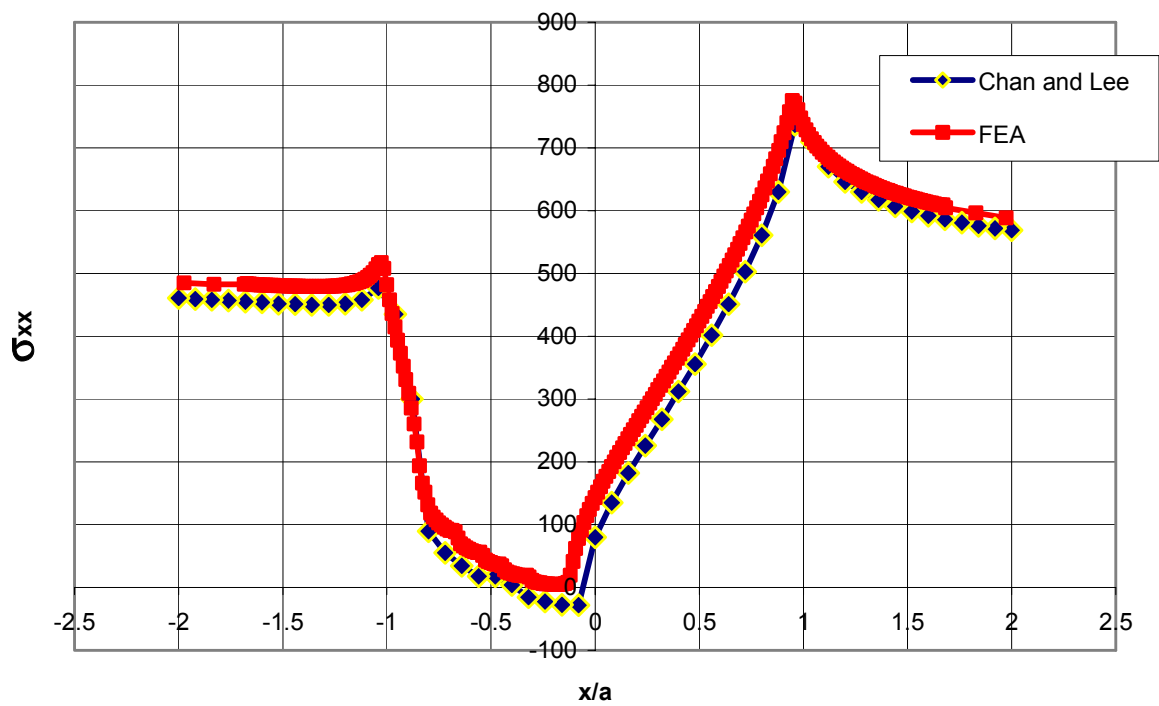
Figure 4.2. Normal Stress in the X-Direction Along the Contact Surface.

Figure 4.3. Comparison of Elevated Temperature Fretting Fatigue And Plain Fatigue
Data using SWT Parameter

Figure 4.4. Comparison of Room and Elevated Temperature Plain Fatigue Data using SWT Parameter.

Figure 4.5. Comparison of Room and Elevated Temperature Fretting Fatigue Data using $\Delta \tau_{crit,effective}$ Parameter.

Figure 4.6. Comparison of Room and Elevated Temperature Fretting Fatigue Data using $\Delta\tau$ Parameter.
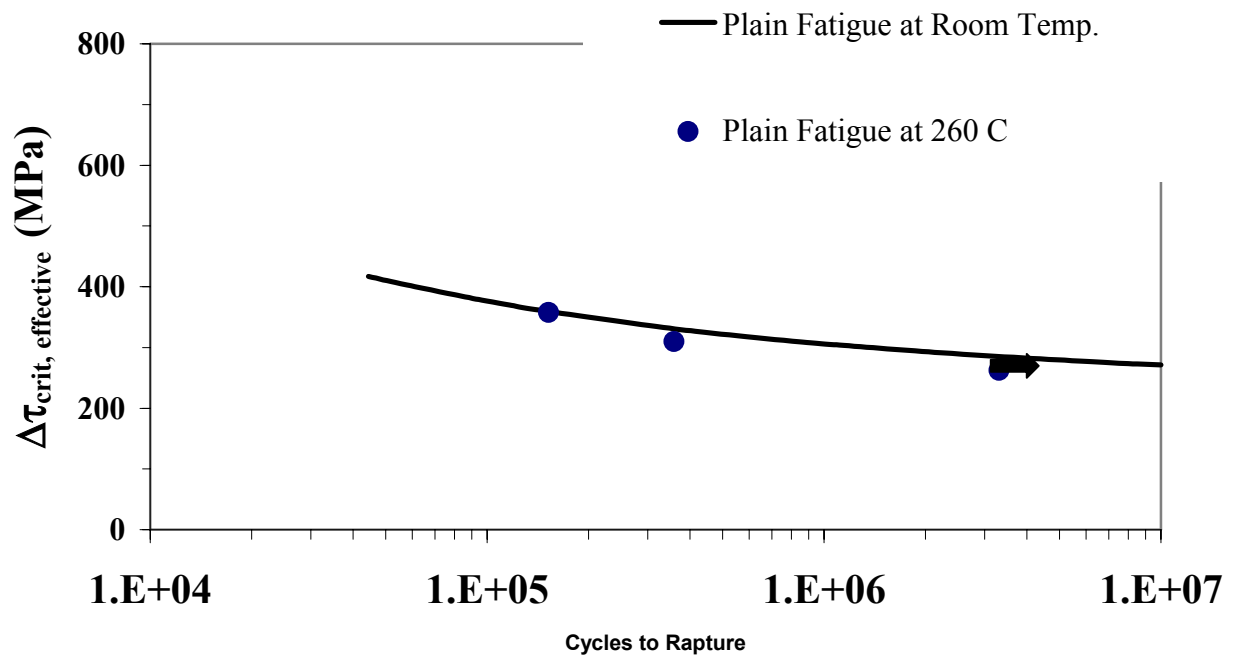
Figure 4.7. Comparison of Room and Elevated Temperature Plain Fatigue Data using $\Delta\tau_{crit,effective}$ Parameter.

Figure 4.8. Comparison of Room and Elevated Temperature Plain Fatigue Data using $\Delta\tau$ Parameter.
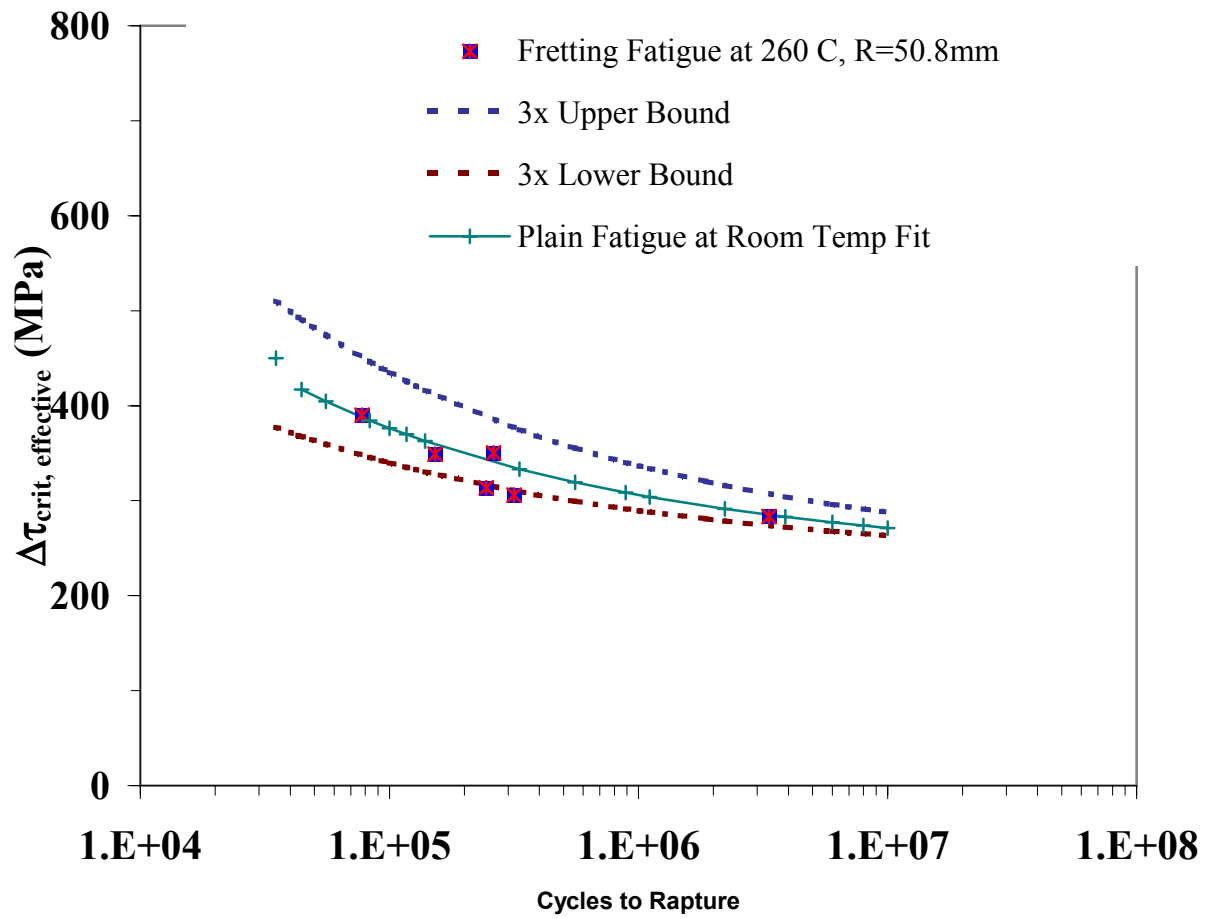
Figure 4.9. Scatter Band of Room Temperature Plain Fatigue Data using $\Delta\tau_{crit,effective}$ Parameter.
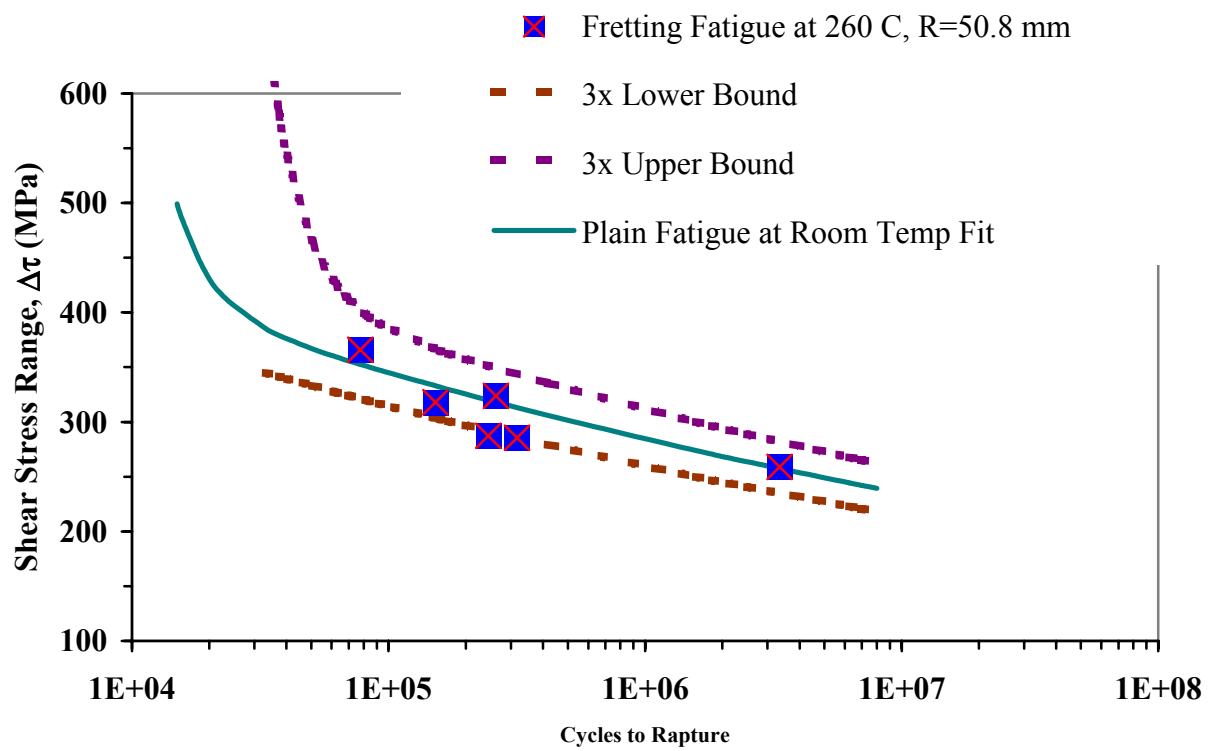
Figure 4.10. Scatter Band of Room Temperature Plain Fatigue Data using Shear Stress
Range Parameter.
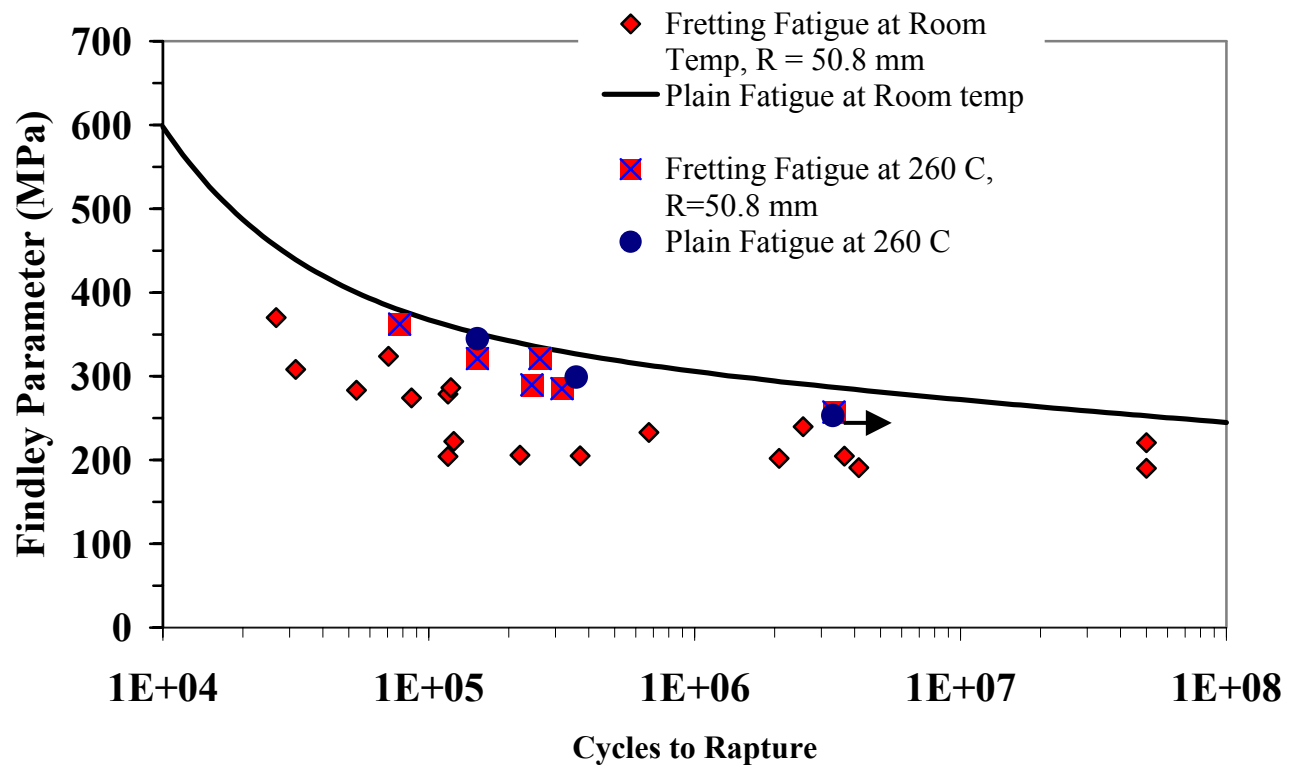
Figure 4.11. Comparison of Room and Elevated Temperature Fretting Fatigue Data using Findley Parameter.
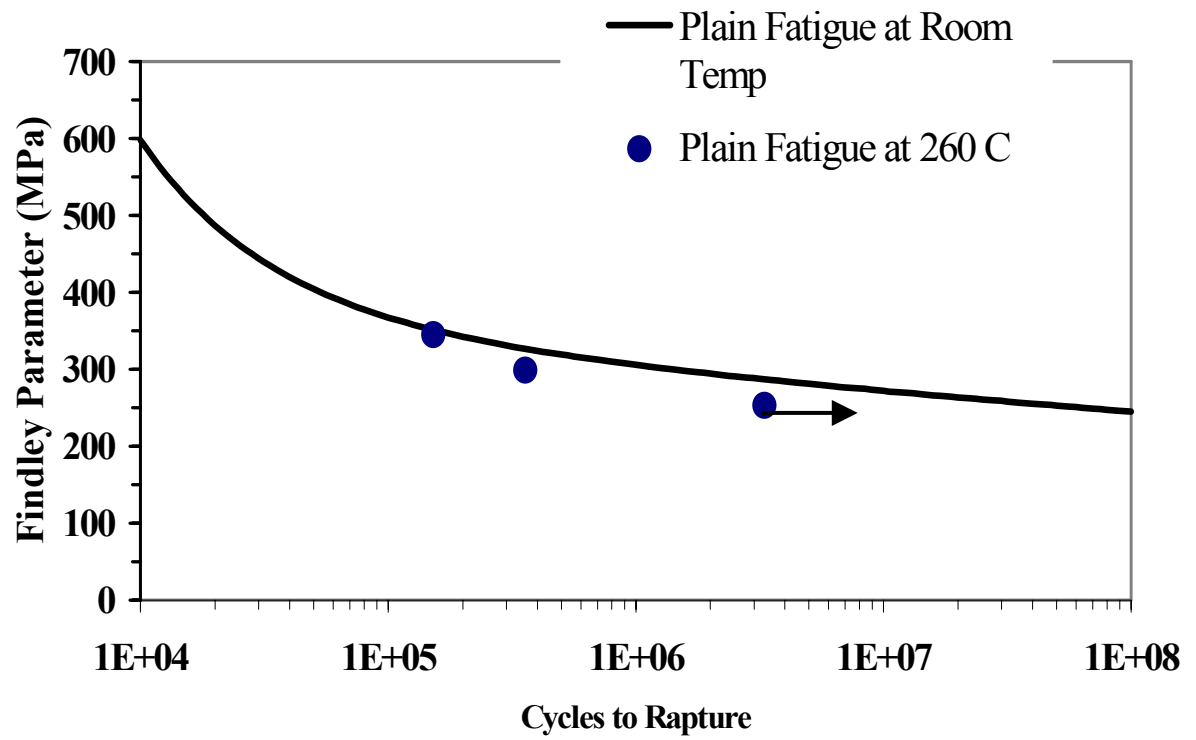
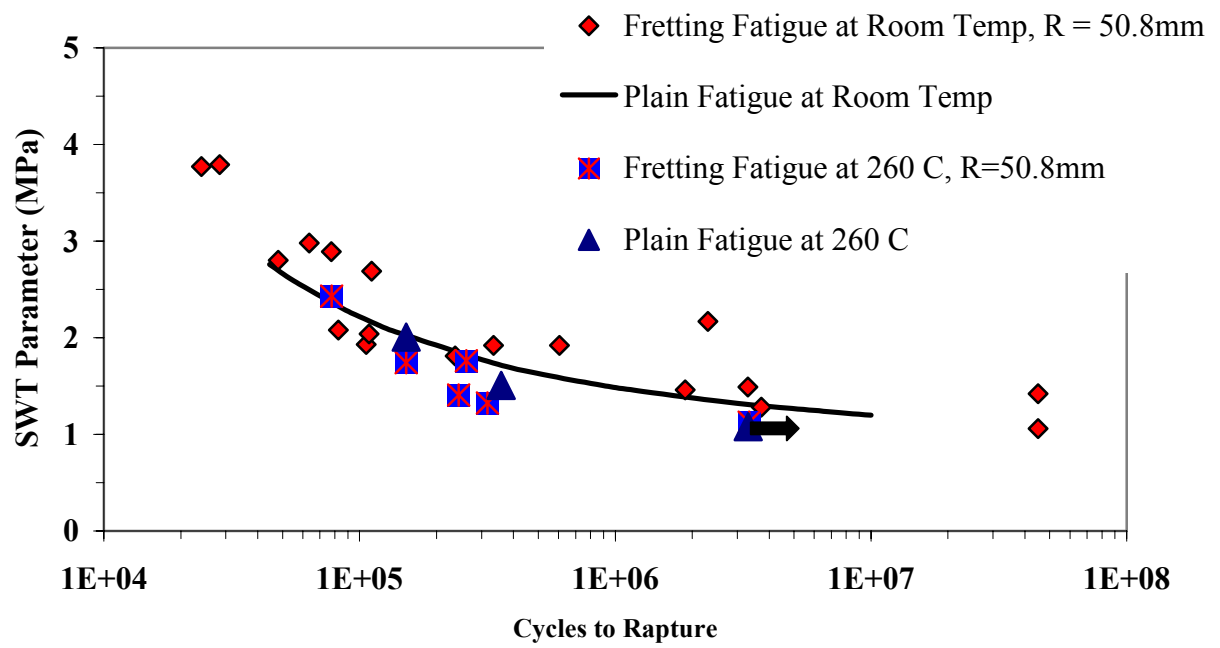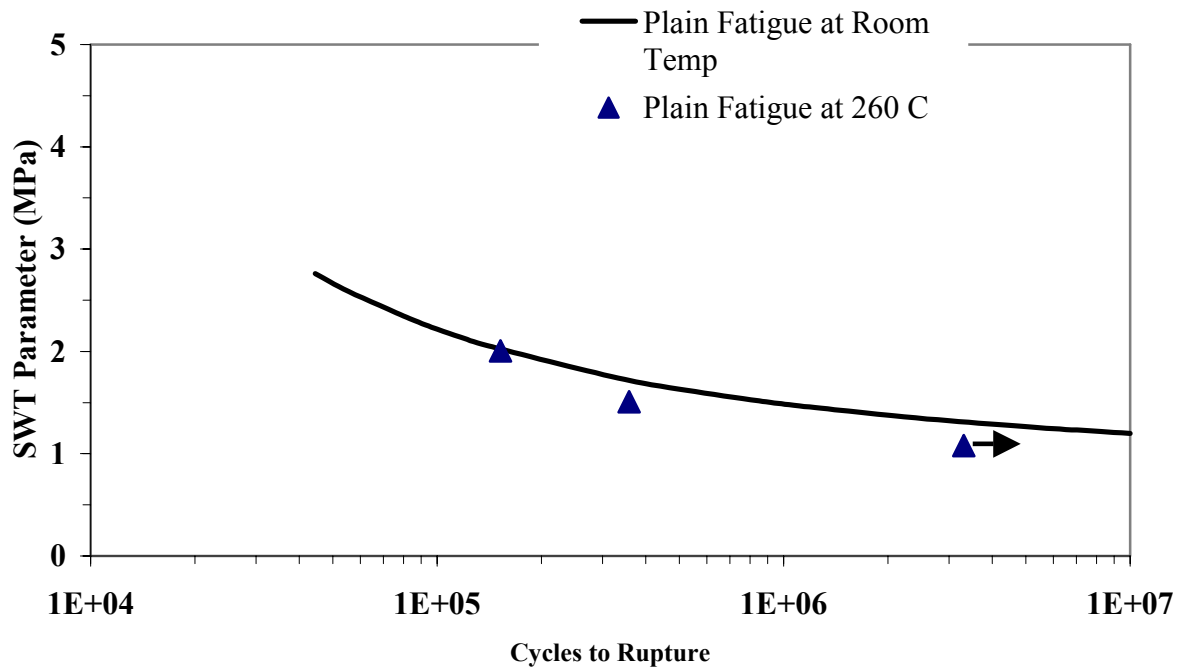Figure 4.12. Comparison of Room and Elevated Temperature Plain Fatigue Data using Findley Parameter.
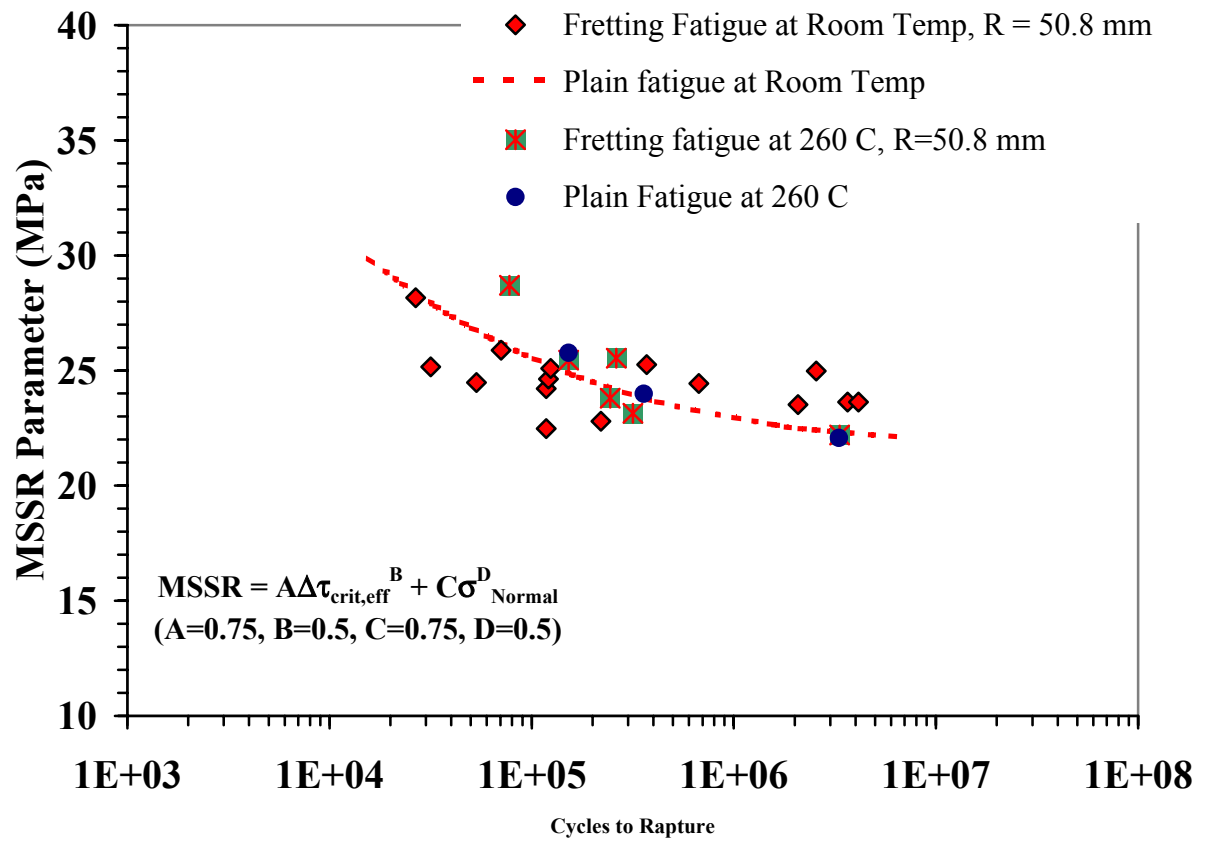
Figure 4.13. Comparison of Room and Elevated Temperature Fretting Fatigue Data using MSSR Parameter.

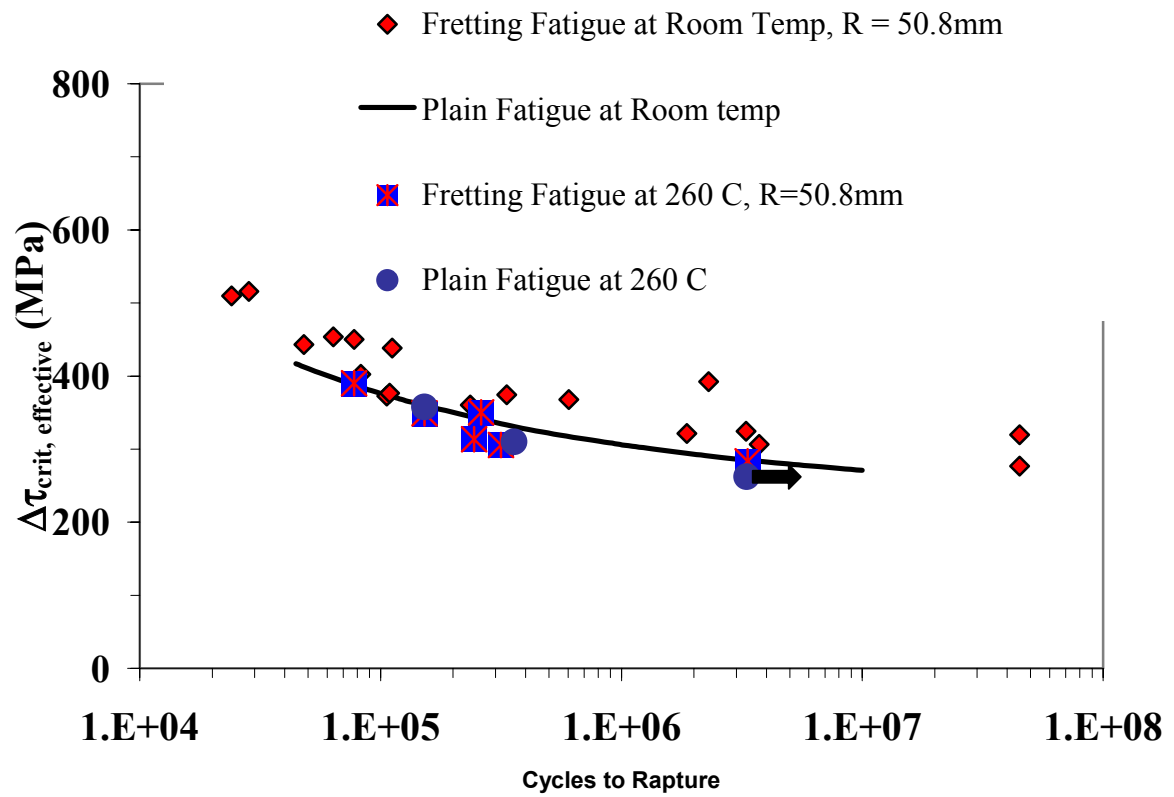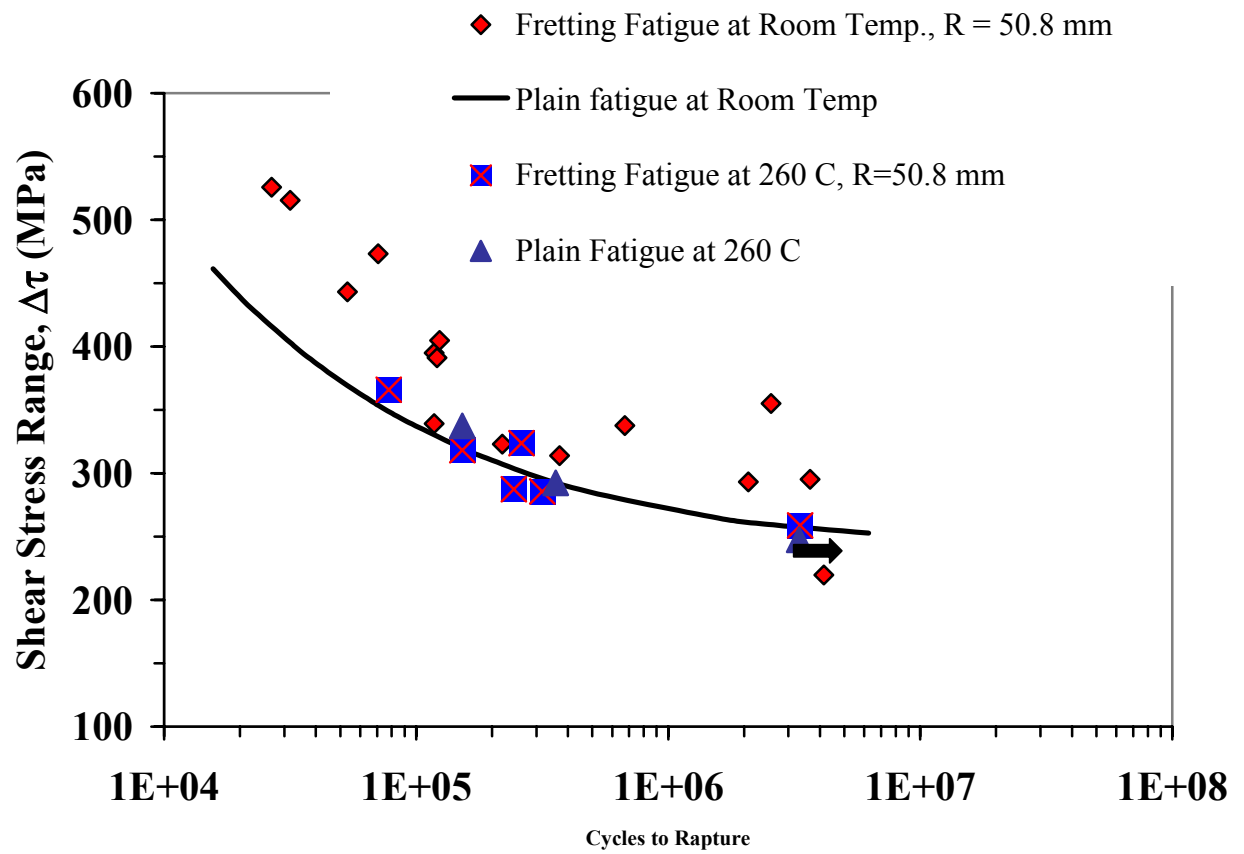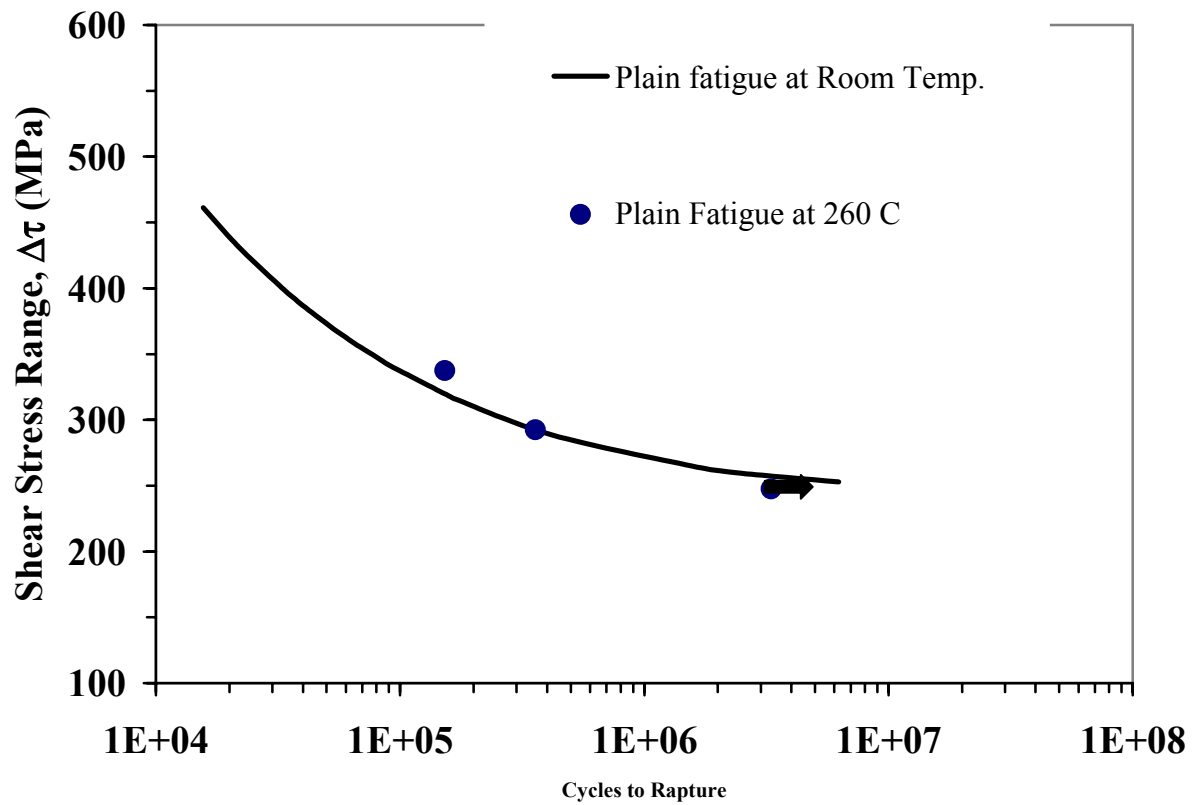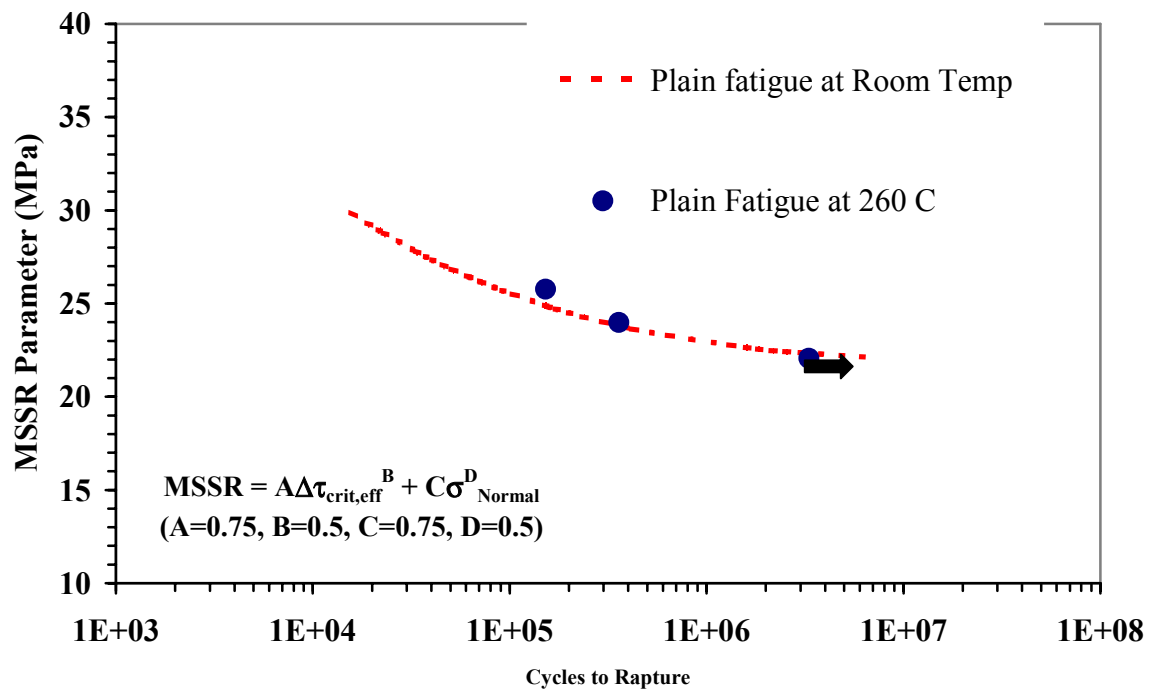Figure 4.14. Comparison of Room and Elevated Temperature Plain Fatigue Data using MSSR Parameter.
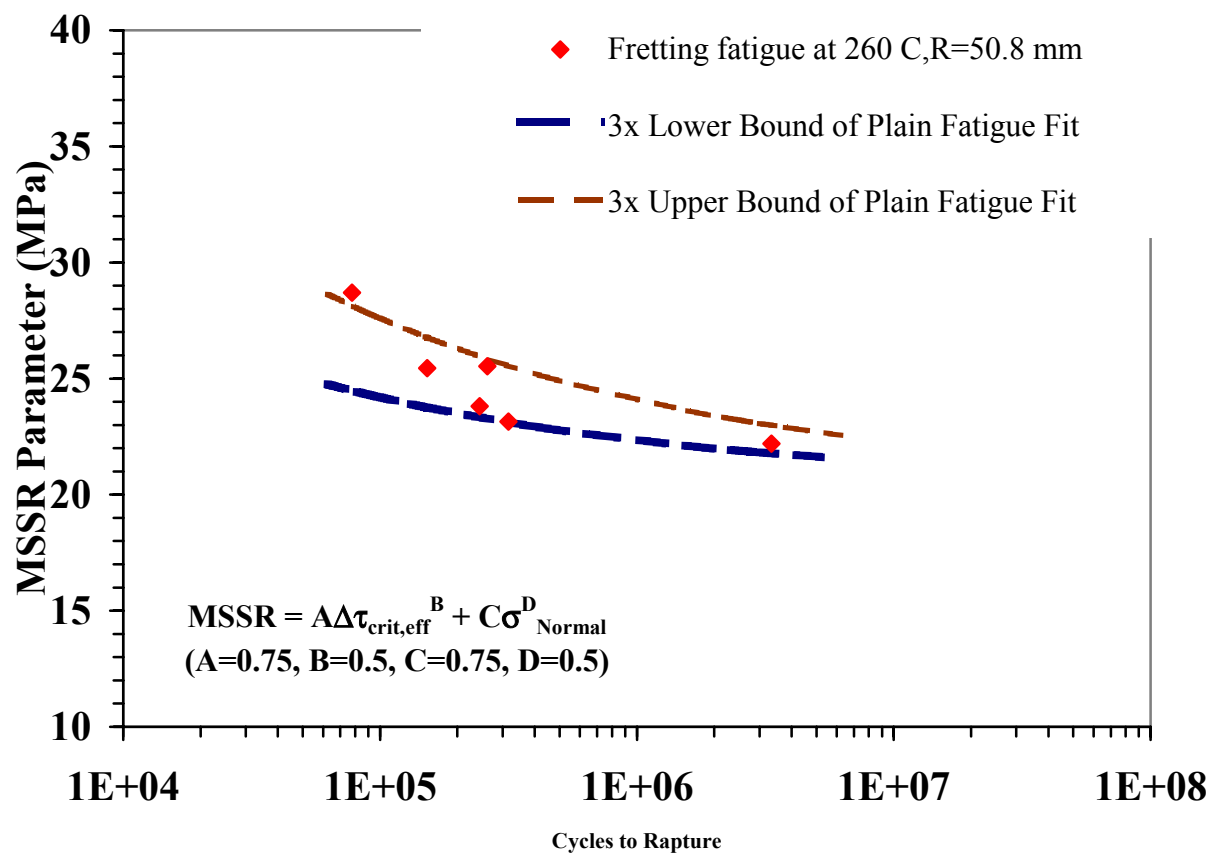
Figure 4.15. Scatter Band of Room Temperature Plain Fatigue Data using MSSR Parameter.

Table 4.1. Smith-Watson-Topper Parameter Analysis Results for Elevated Temperature Fretting Fatigue.

Specimen Number	N_f	SWT MPa	Orientation Degree	Crack Location a
10	3338962	1.126243	-0.4	0.946549
3	77732	2.429163	0.1	0.946549
5	261755	1.763096	-0.4	0.946549
6	244338	1.408467	-0.3	0.946549
7	152341	1.740607	-0.3	0.946549
8	316513	1.325973	0.1	0.946549

Table 4.2. $\Delta\tau$, $\Delta\tau_{crit,effective}$ and MSSR Parameters Analysis Results for Elevated Temperature Fretting Fatigue.

Specimen Number	N_f	$\Delta\tau$ MPa	$\Delta\tau_{crit,effective}$ MPa	σ_{max} MPa	MSSR MPa	Orientation Degree	Crack Location a
10	3338962	258.9643	283.3012	162.9832	22.19853	44.1	0.946549
3	77732	366.0293	390.0128	342.8864	28.69945	44	0.946549
5	261755	323.7291	350.2336	234.8775	25.53018	43.9	0.946549
6	244338	287.3413	313.6537	196.7834	23.80367	41.5	0.946549
7	152341	318.1462	348.827	232.6153	25.44648	44.5	0.946549
8	316513	285.5364	305.785	179.746	23.17024	42	0.946549

Table 4.3. Findley Parameter Analysis Results for Elevated Temperature
Fretting Fatigue.

		FP	Orientation	Crack Location
Specimen Number	N_f	MPa	Degree	a
10	3338962	257.567	-22.1	0.946549
3	77732	362.2306	-25.5	0.946549
5	261755	321.3124	-23.1	0.946549
6	244338	289.9566	-21.7	0.946549
7	152341	321.0371	-22.3	0.946549
8	316513	285.46	-19.9	0.946549

Table 4.4. Parameter Analysis Results for Elevated Temperature Plain Fatigue.

	SWT	$\Delta\tau$	$\Delta\tau_{crit,effective}$	FP	MSSR	Orientation
N_f	MPa	MPa	MPa	MPa	MPa	Degree
3307000	1.079244	247.5	262.266	253.024	22.07028	45
152323	2.006858	337.5	357.635	345.033	25.77254	45
358243	1.507373	292.5	309.951	299.028	23.99293	45

V. Summary and Conclusions

The purpose of this thesis is to investigate the fretting fatigue behavior of a titanium alloy, Ti-6Al-4V at elevated temperature. In this study, main motivation is to get the elevated temperature fretting fatigue life data of titanium alloy Ti-6Al-4V, and develop a parameter that can predict number of cycles to crack initiation, crack location, and crack orientation. For this reason, in order to obtain elevated temperature fretting fatigue data in both the low cycle and high cycle fatigue regimes, several tests with different applied loads are tested. Experimental studies show that $260\,^{\circ}C$ temperature does not have detrimental effect on the fretting fatigue behavior of this material, because elevated temperature fretting fatigue life data lie very close to room temperature fretting fatigue life data. The salient features of the elevated temperature fretting fatigue experiments are modeled and analyzed with finite element analysis. The results of the finite element analyses are used to formulate and evaluate several fatigue parameters. The fatigue parameters for the elevated temperature fretting fatigue experiments are then compared to elevated temperature plain fatigue parameters as well as to room temperature fretting fatigue and plain fatigue parameters.

The fretting fatigue specimens are examined to determine the location of crack initiation and the crack orientation along the contact surface. It is found that crack location occurs near the trailing edge of contact or near x/a = 1.0, and angle of orientation, θ, along the contact surface is about $\theta = -45°$. The fatigue parameters are evaluated on their ability to predict these observations. Based on the comparison between

88

the fretting fatigue, the plain fatigue data and the correlation of the experimental observations, fretting fatigue crack initiation is found to occur in response to the critical plane shear stress amplitude. Following topics summarize the work that has been done to arrive these conclusions.

Experimental Studies and Results

In this part of the research, elevated temperature fretting fatigue and plain fatigue experiments are performed to generate the data needed to establish the crack initiation behavior of a titanium alloy, Ti-6Al-4V. The following paragraphs summarize the techniques that are used in this research and conclusions that are arrived in this part of the research.

To generate the elevated temperature fretting fatigue and plain fatigue data, an experimental configuration is developed. Two infrared spot heaters are used to reach the target temperature in the contact region and at the center of the specimen for plain fatigue, then the results are checked by using handbook data for this material, and it is seen that the data generated is appropriate.

The results of these experiments are as follows: first of all, experiments indicate that $260\ °C$ temperature doesn't change the properties of this material. It is seen that the life reduction due to the elevated temperature fretting fatigue is same as the room temperature fretting fatigue. Second the crack location is determined to be near the trailing edge of the contact or near x/a = 1.0. Further, the crack orientations along the contact surface are found to be approximately $45°$.

FEA and Fretting Fatigue Parameter Evaluation and Results

In order to simulate the complex interaction that occurs in the fretting fatigue tests, finite element analyses are required in this study. The analytical methods have the limitation since they assume that the contacting bodies have infinite boundaries, but the fretting fatigue specimen used in the experimental portion of this study has finite boundaries. However, the finite element model with an infinitely wide specimen is compared to these analytical methods in order to validate the model. The finite element model output, such as normal stress in the x-direction, contact width and maximum pressure along the contact surface, are determined to be at least 95% of those from the alternative analytical models. Therefore, the finite element model is determined to be accurate representation of the fretting fatigue experimental configuration.

Finite element model results are used to calculate several fretting fatigue parameters, and these parameters are evaluated on their ability to predict the number of cycles to crack initiation, the crack location, and the orientation of the crack along the contact interface. Furthermore, room and elevated temperature plain and fretting fatigue data are compared to determine the limitations of the evaluated fatigue parameters. The following is a very short summary of this portion of the research.

1. Smith-Watson-Topper critical plane parameter predicts the cycles to fretting fatigue crack initiation and crack location, which are in agreement with their experimental counterparts. However, this parameter predicts the crack orientation which is different than experimental observation, also this parameter is based on only normal stress on the critical plane.

2. Shear-cracking based critical plane parameter, $\Delta\tau_{crit,effective}$, predicts the cycles to fretting fatigue crack initiation, crack initiation location and crack orientation which are in agreement with their experimental counterparts. This parameter can be used to predict these fretting fatigue mechanisms for elevated temperature fretting fatigue. However, as mentioned before this parameter is based on only shear stress on the critical plane, and a previous study [34] points out the limitations of this parameter with a large variation of geometry and peak normal stress. Therefore, a fretting parameter, which is a combination of shear and normal stresses on a critical plane, can describe the fretting fatigue of Ti-6Al-4V better than a fretting parameter that is based on only shear stresses or normal stresses.

3. Findley parameter, a critical plane approach involving both normal and shear stresses, predicts the crack location satisfactorily. However, it does not predict the crack orientation satisfactorily and in addition Findley parameter does not give a good relationship for fretting fatigue life relationships. For this reason this parameter cannot be used to predict the fretting fatigue crack initiation life, location and orientation at elevated temperature.

4. A modified version of shear stress range parameter, MSSR, involving both normal and shear stresses (or both tensile and shear cracking) predicts the cycles to fretting fatigue crack initiation, crack initiation location and crack orientation which are in agreement with their experimental counterparts. Also elevated temperature fretting fatigue data for MSSR parameter falls into scatter band of room temperature plain fatigue data. This clearly indicates that this parameter can

be used to predict the fretting fatigue life from the plain fatigue data in conjunction with an analysis. Further, this modified parameter explicitly includes the effects of the shear stress as well as normal stress as should be the case for multi-axial fatigue loading condition. Finally the MSSR (or a similar) parameter may be used to predict the fretting fatigue life from the plain fatigue data in conjunction with an analysis.

Future Work

In this study the test temperature is 260 $°C$, and the main conclusion is that the life reduction due to the elevated temperature fretting fatigue is same as the life reduction due to the room temperature fretting fatigue. However, the situations at higher temperatures are unknown. For this reason, higher temperature studies should be done, and fretting fatigue behavior of Ti-6Al-4V at higher temperatures with different fretting fatigue configurations should be understood in order to have a complete picture of fretting fatigue research.

<u>Appendix A: Work At Laboratory</u>

Since most of the time was spent at laboratory, it was necessary to mention the work that was done at laboratory. The work done at laboratory can be divided into two parts: one part on fretting fatigue under elevated temperature and one part on plain fatigue under elevated temperature.

<u>Fretting Fatigue Studies</u>

First of all, fretting fixture in our study was a new test device. For this reason, it took more time to get a good alignment with this fixture. Most of the time, which was about one month, was spent on correcting the alignment. After this, studies concerning the temperature profile on the specimen were done. During this time, some problems were experienced related to thermocouple attachment. By using indirect method to control the temperature on the specimen, this problem was overcome. However, another problem concerning the normal load was experienced. By applying some small adjustments on the fixture, this problem was overcome too. Finally, after all these problems some fretting fatigue at elevated temperature data were obtained.

<u>Plain Fatigue Studies</u>

Difficulties that were encountered at these studies were related to elevated temperature. First, since the thermocouple was not welded to the specimen, indirect

method was tried again. Also different lamps were used first for plain fatigue experiments. However, some very early failures were experienced.

For this reason, another method was tried to attach the thermocouple to the specimen, which was using high temperature epoxy. Further, the spot heaters of fretting fatigue studies were used here again. Finally, three experiment points were obtained with this method.

Appendix B: Temperature Analysis in ABAQUS

The temperature of the analysis can be defined in ABAQUS by using the predefined fields option. Predefined fields are defined within a step by the *FIELD, *PRESSURE STRESS, and *TEMPERATURE options. Here, the use of the *TEMPERATURE option is described to specify the values of predefined fields during an analysis.

Temperature is a time-dependent (not solution-dependent) field that exists over the spatial domain of the model [40]. It can be defined:

- By using the data line format,

- By reading an ABAQUS results file generated during a previous analysis, or

- In a user subroutine.

Field variables can also be made solution dependent, which makes it possible for the user to introduce additional nonlinearities in the ABAQUS material models. In this study the temperature difference between the temperature field defined by the *TEMPERATURE option and the temperature field defined by the *INITIAL CONDITIONS option. An example of these options can be shown as follows:

**Initial temperature value

*INITIAL CONDITIONS, TYPE=TEMPERATURE

NPLATE, 70.0

NCYL, 70.0

NSPRPAD, 70.0

Here NPLATE, NCYL, and NSPRPAD are group nodes that define the bodies that are discussed in Chapter IV, and note that temperature is defined in Fahrenheit. For *TEMPERATURE option, the example is as follows:

*TEMPERATURE

NPLATE, 500.0, 0.0

NCYL, 500.0, 0.0

NSPRPAD, 500.0, 0.0

Bibliography

1. Birch, P.R. <u>A Study of Fretting Fatigue in Aircraft Components.</u> MS thesis, Department of Materials Science and Engineering, USAF Academy, May 8 1998.

2. Nishioka K. and Hirakawa K., <u>"Fundamental Investigations into Fretting Fatigue"</u> Part 2, Bulletin of JSME, Vol. 12, 397-407, 1969.

3. Chivers, T. C. <u>"Fretting Fatigue and Contact Conditions - A Rational Explanation of Palliative Behavior"</u> Institution of Mechanical Engineers, Proceedings, Part C Mechanical Engineering Science 325-337, United Kingdom, 1985.

4. Broszeit, E<u>. "Fretting Fatigue Testing With a Fretting Bridge Equipment Stress Analysis"</u> Proceedings of the Fifth International Conference on Titanium 2179-2186, Munich, West Germany, September 10-14, 1984.

5. Friedrich, K. <u>"Fretting Fatigue Studies on Carbon Fibre/Epoxy Resin Laminates. I - Design of a Fretting Fatigue Test Apparatus"</u> Composites Science and Technology 19-34 Vol. 30, no. 1, 1987.

6. Li, Dongzi <u>"Fretting Damage in Aircraft Industry and The General Situation of Research"</u> Acta Aeronautica et Astronautica Sinica A 535-A 542. (In Chinese, with abstract in English), CHINA, 1987.

7. Sakata, H. <u>"An Application of Fracture Mechanics to Fretting Fatigue Analysis"</u> Proceedings of the International Conference, 303-313, Amsterdam and New York, North-Holland, 1987.

8. Hattori, Toshio <u>"Fretting Fatigue Analysis Using Fracture Mechanics"</u> JSME International Journal, 100-107, JAPAN, Jan. 1988.

9. He, Mingjian <u>"Fretting Fatigue - Stress Distribution and Prediction of Crack Location in Dovetail Joints"</u> Journal of Aerospace Power Vol. 4, 205-208, CHINA, July 1989.

10. He, Mingjian <u>"Fretting Fatigue in Component - The Feature in Circumferential Dovetail Joints"</u> Acta Aeronautica et Astronautica Sinica Vol. 12, p. B307-B310, CHINA, 1991.

11. Adibnazari, Saeed. <u>Investigation of Fretting Fatigue Mechanisms on 7075-T6 Aluminum Alloy and Ti-6Al-4V Titanium Alloy;</u> Ph.D. Thesis, Utah Univ., Salt Lake City, 1991.

12. Abidnazari, Saeed. <u>"A Fretting Fatigue Normal Pressure Threshold Concept"</u>Wear, Switzerland, 1993.

13. Szolwinski, M. P.; Farris, T. N. "Fretting Fatigue Crack Initiation - Aging Aircraft Concerns" AIAA/ASME/ASCE/AHS/ASC Structures, Structural Dynamics, and Materials Conference, Technical Papers. 2173-2179, Washington, DC, 1994.

14. Hoeppner, David. "Literature Review and Preliminary Studies of Fretting and Fretting Fatigue Including Special Applications to Aircraft Joints,Final Report." Report No.: AD-A280310; DOT/FAA/CT-93/2,1994.

15. Switek, Wieslaw. "Fretting fatigue Strength of Specimens Subjected to Combined Axial and Transversal Loading." 208-223, Proceedings of the Symposium, Denver, CO, 1997.

16. Szolwinski, Matthew. "Comparison of Fretting Fatigue Crack Nucleation Experiments to Multi-Axial Fatigue Theory Life Predictions" Proceedings of the Symposia, 1997 ASME International Mechanical Engineering Congress and Exposition, 449-457, Dallas, TX, Nov. 16-21, 1997.

17. Hattori, T. "Initiation and Propagation Behavior of Fretting Fatigue Cracks" Proceedings of the 3rd International Conference on Contact Mechanics, 183-192, Madrid, Spain, July 1997.

18. Iyer, K. and Others. "Effects of Cyclic Frequency and Contact Pressure on Fretting Fatigue Under Two-Level Block Loading" Fatigue and Fracture of Engineering Materials and Structures (ISSN 8756-758X), Vol.. 23, no. 4, p. 335-346. United States, 2000.

19. Lykins, Christopher D. An Investigation Of Fretting Fatigue Crack Initiation Behavior of Titanium Alloy Ti-6Al-4V. Air Force Institute of Technology, Wright-Patterson AFB OH, December 1999.

20. Ruiz C., Boddington P. and Chen K. "An Investigation of Fatigue and Fretting in Dovetail Joint" Experimental Mechanics, Vol. 24, 208-217, 1984.

21. Waterhouse, R.B. "Metallurgical Changes in The High Temperature Fretting of Ni and Ti Alloys" Report No: AD A 046002, Contract Number DAJA 37-75-R-0649, 1977.

22. Elder, J. E. "Surface Property Improvement in Titanium Alloy Gas Turbine Components Through Ion Implantation" In AGARD, High Temperature Surface Interactions 11 p (SEE N90-28698 23-26) Ottawa, Ontario, 1989.

23. Mutoh, Y. "Fretting Fatigue at Elevated Temperatures in Two Steam Turbine Steels" Fatigue and Fracture of Engineering Materials and Structures, Vol. 12:5,409-421, 1989.

24. Schaefer, Rainer. "Fretting Fatigue Strength of Ti-6Al-4V at Room and Elevated Temperatures " In AGARD, High Temperature Surface Interactions 15 p (SEE N90-28698 23-26), Germany, 1989.

25. Waterhouse, R. B. "Fretting Wear and Fretting Fatigue at Temperatures up to 600 °C " In AGARD, High Temperature Surface Interactions 12 p (SEE N90-28698 23-26), United Kingdom, 1989.

26. Dai, Zhen-Dong. "Experimental Studies on Fretting Fatigue of Stainless Steel and Titanium Alloy" Acta Aeronautica et Astronautica Sinica (ISSN 1000-6893), Vol. 20, no. 3, p. 245-248, 1999, China.

27. Hills D. and Nowell D. "Mechanics of Fretting Fatigue" Kluwer Academic Publishers, Netherlands, 1994.

28. Fellows L.,Nowell D, Hills D. "Contact Stresses in a Moderately Thin Strip (with Particular Reference to Fretting Experiments)" Wear, Vol. 185,235-238, 1995.

29. Chan K. and Lee Y. "Ruiz Program" South West Research Institute, Personal Communication, 1998.

30. Military Handbook-5E,5-86, U.S. Department of Defense, 1987.

31. ABAQUS Standard User's Manual Vol. 2., Hibbit, Karlsson and Sorensen, Inc. 1995.

32. Robert D. Cook and others. Concepts And Applications of Finite Element Analysis. New York: Hamilton Printing Company, 1989.

33. Research INC. Model 4085 Infrared Spot Heater Instruction Manual. Publication No. 098919-001 Rev.A. Minnesota August 1998.

34. Shantanu A. Namjoshi and Others. Fretting Fatigue Crack Initiation Mechanism in Ti-6Al-4V. Air Force Institute of Technology, Wright-Patterson AFB OH, December 2000.

35. P. Mc Veigh and T. Farris. "Finite Element Analysis of Fretting Stresses" Journal of Tribology, 1997, Vol. 119, 797-801.

36. A. Krgo, A. R. Kallmeyer, and P. Kurath, "Evaluation of HCF Multiaxial Fatigue Life Prediction Methologies for Ti-6Al-4V", Proceeding of the 5th National Turbine Engine High Cycle Fatigue Conference, Arizona, 2000.

37. C. D. Lykins, S. Mall and V. K. Jain, "A Shear Stress Based Parameter for Fretting Fatigue Crack Initiation", Fatigue and Fracture of Engineering Materials and Structures (in press).

38. K. Walker, "The Effect of Stress Ratio During Crack Propagation and Fatigue for 2024-T3 and 7075-T6 Aluminum", Effects of Environment and Complex Load History on Fatigue Life. American Society for Testing and Materials, West Conshohocken, PA. STP 462, pp. 1-14, 1970.

39. W. N. Findley, "Fatigue of Metals Under Combinations of Stresses", Transactions, ASME, Vol. 79, pp. 1337-1348, 1957.

40. ABAQUS Standard User's Manual Vol. 3., Hibbit, Karlsson and Sorensen, Inc. 1995.

Vita

      Lieutenant Onder Sahan was born in Adana, Turkiye. He graduated from Maltepe Military High School in Izmir in 1995. He entered undergraduate studies at Turkish Air Force Academy in the same year. He graduated with a Bachelor of Science degree in Aeronautical Engineering in 1999.

      His first assignment was at Gaziemir, Izmir as a student in Explosive Ordnance Disposal Training in 1999. Upon graduation he entered the Graduate School of Engineering and Management, Air Force Institute of Technology.

REPORT DOCUMENTATION PAGE

The public reporting burden for this collection of information is estimated to average 1 hour per response, including the time for reviewing instructions, searching existing data sources, gathering and maintaining the data needed, and completing and reviewing the collection of information. Send comments regarding this burden estimate or any other aspect of the collection of information, including suggestions for reducing this burden to Department of Defense, Washington Headquarters Services, Directorate for Information Operations and Reports (0704-0188), 1215 Jefferson Davis Highway, Suite 1204, Arlington, VA 22202-4302. Respondents should be aware that notwithstanding any other provision of law, no person shall be subject to an penalty for failing to comply with a collection of information if it does not display a currently valid OMB control number.
PLEASE DO NOT RETURN YOUR FORM TO THE ABOVE ADDRESS.

1. REPORT DATE (DD-MM-YYYY)	2. REPORT TYPE	3. DATES COVERED (From – To)
26-03-2002	**Master's Thesis**	Sep 2000 – Mar 2002

4. TITLE AND SUBTITLE	5a. CONTRACT NUMBER
FRETTING FATIGUE BEHAVIOR OF A TITANIUM ALLOY TI-6AL-4V AT ELEVATED TEMPERATURE	5b. GRANT NUMBER
	5c. PROGRAM ELEMENT NUMBER

6. AUTHOR(S)	5d. PROJECT NUMBER
Onder Sahan, Lieutenant, TUAF	5e. TASK NUMBER
	5f. WORK UNIT NUMBER

7. PERFORMING ORGANIZATION NAMES(S) AND ADDRESS(S)	8. PERFORMING ORGANIZATION REPORT NUMBER
Air Force Institute of Technology Graduate School of Engineering and Management (AFIT/EN) 2950 P Street, Building 640 WPAFB OH 45433-7765	AFIT/GAE/ENY/02-11

9. SPONSORING/MONITORING AGENCY NAME(S) AND ADDRESS(ES)	10. SPONSOR/MONITOR'S ACRONYM(S)
AFRL / MLLMN Attn: Dr. Jeffrey Calcaterra 2230 Tenth Street Suite 1 DSN: 785-1360 WPAFB, OH 45433-7817 email: Jeffrey.Calcaterra@wpafb.af.mil	11. SPONSOR/MONITOR'S REPORT NUMBER(S)

12. DISTRIBUTION/AVAILABILITY STATEMENT

APPROVED FOR PUBLIC RELEASE; DISTRIBUTION UNLIMITED.

13. SUPPLEMENTARY NOTES

14. ABSTRACT

The purpose of this research is to investigate the fretting fatigue behavior of the titanium alloy Ti-6Al-4V at elevated temperature. This study includes both elevated temperature fretting and plain fatigue behavior of this material. The experiments are done at 260 $^{\circ}C$. Crack initiation location and crack initiation orientation is observed and fretting and plain fatigue life data of the specimens from these tests are obtained. Fatigue parameters capable of predicting the number of cycles to specimen failure, the crack location and the crack orientation along the contact surface are analyzed. The parameters are calculated by using the computed stresses and strains obtained from the finite element analysis. The mechanisms responsible for the fretting fatigue crack initiation are determined. The effect of elevated temperature is examined by comparing room and elevated temperature fretting and plain fatigue data.

15. SUBJECT TERMS
Fretting Fatigue, Plain Fatigue, Ti-6Al-4V, Elevated Temperature, Fretting Parameters

16. SECURITY CLASSIFICATION OF:			17. LIMITATION OF ABSTRACT	18. NUMBER OF PAGES	19a. NAME OF RESPONSIBLE PERSON Shankar Mall
a. REPORT U	b. ABSTRACT U	c. THIS PAGE U	UU	116	19b. TELEPHONE NUMBER (937) 255-3636, ext 4587; e-mail: Shankar.Mall@wpafb.af.mil